REVIEW

OPEN ACCESS

Untethered miniature robots for minimally invasive thrombus treatment: From bench to clinical trials

Qinglong Wang,[1,3] Fangling Zhao,[2] Ben Wang,[4,*] Kai Fung Chan,[5,6] Bonaventure Yiu Ming Ip,[7] Thomas Wai Hong Leung,[7] Xin Song,[8,*] Li Zhang,[1,3,6,9,10,*] and Jue Xie[2,*]

*Correspondence: benwang@szu.edu.cn (B.W.); xinsong@cityu.edu.hk (X.S.); lizhang@cuhk.edu.hk (L.Z.); zyyyxj2011@zju.edu.cn (J.X.)

Received: September 24, 2024; Accepted: March 6, 2025; Published Online: March 11, 2025; https://doi.org/10.1016/j.xinn.2025.100874

GRAPHICAL ABSTRACT

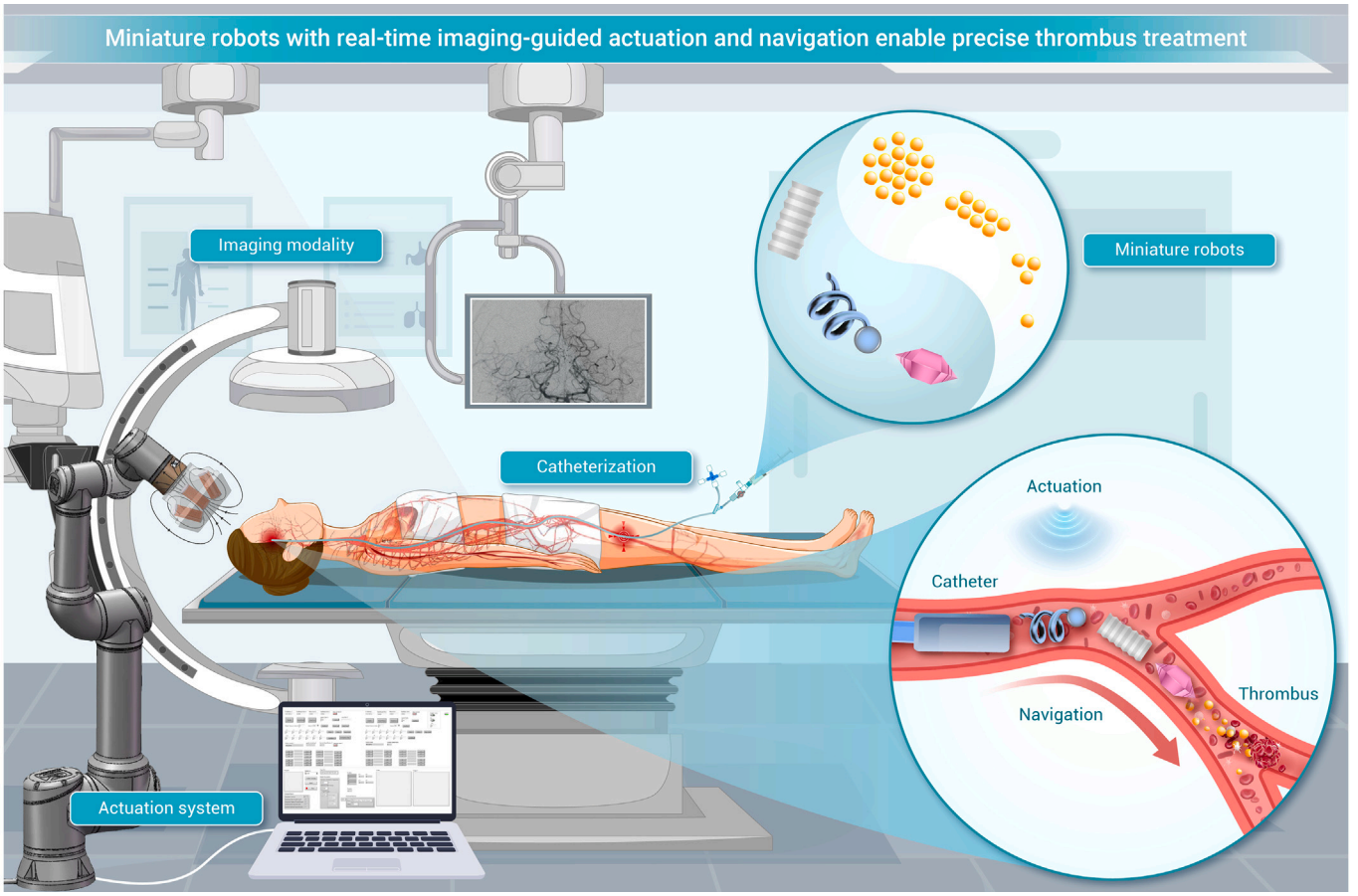

PUBLIC SUMMARY

- Ischemic stroke is a leading cause of death, with thrombectomy and thrombolysis being common treatments.
- Limited catheter accessibility and the serious side effects of thrombolytic drugs are the main challenges.
- Untethered miniature robots (MRs) enable precise therapy with minimized side effects.
- This work explores the design principles, current challenges, and prospects of MRs for thrombus treatment.

OPEN ACCESS

REVIEW

The Innovation

Untethered miniature robots for minimally invasive thrombus treatment: From bench to clinical trials

Qinglong Wang,[1,3] Fangling Zhao,[2] Ben Wang,[4,*] Kai Fung Chan,[5,6] Bonaventure Yiu Ming Ip,[7] Thomas Wai Hong Leung,[7] Xin Song,[8,*] Li Zhang,[1,3,6,9,10,*] and Jue Xie[2,*]

[1]Department of Mechanical and Automation Engineering, The Chinese University of Hong Kong, Shatin N.T., Hong Kong SAR 999077, China
[2]Department of Blood Transfusion, The First Affiliated Hospital, Zhejiang University School of Medicine, Hangzhou 310003, China
[3]Shenzhen Research Institute, The Chinese University of Hong Kong, Shenzhen 518000, China
[4]College of Chemistry and Environmental Engineering, Shenzhen University, Shenzhen 518055, China
[5]Li Ka Shing Institute of Health Sciences, The Chinese University of Hong Kong, Shatin N.T., Hong Kong SAR 999077, China
[6]Chow Yuk Ho Technology Centre for Innovative Medicine, The Chinese University of Hong Kong, Shatin N.T., Hong Kong SAR 999077, China
[7]Department of Medicine and Therapeutics, Faculty of Medicine, The Chinese University of Hong Kong, Shatin N.T., Hong Kong SAR 999077, China
[8]Department of Biomedical Engineering, City University of Hong Kong, Kowloon Tong, Kowloon, Hong Kong SAR 999077, China
[9]T Stone Robotics Institute, The Chinese University of Hong Kong, Shatin N.T., Hong Kong SAR 999077, China
[10]Department of Surgery, CUHK, Shatin N.T., Hong Kong SAR 999077, China
*Correspondence: benwang@szu.edu.cn (B.W.); xinsong@cityu.edu.hk (X.S.); lizhang@cuhk.edu.hk (L.Z.); zyyyxj2011@zju.edu.cn (J.X.)

Received: September 24, 2024; Accepted: March 6, 2025; Published Online: March 11, 2025; https://doi.org/10.1016/j.xinn.2025.100874

Citation: Wang Q., Zhao F., Wang B., et al., (2025). Untethered miniature robots for minimally invasive thrombus treatment: From bench to clinical trials. The Innovation **6(6)**, 100874.

Untethered miniature robots (MRs) offer a minimally invasive way to address adverse vascular blockages, such as cerebrovascular thromboembolism, myocardial infarction, and pulmonary embolism. This review explores three key questions: what are the design principles of MRs from both engineering and clinical perspectives? How can visible intervention of MRs in three-dimensional (3D) branched vessels be achieved? What is the clinical procedure for treating thrombus using designed MRs? Recent progress in MRs for thrombus removal is summarized, and, more importantly, the pros and cons of MRs are discussed. We also evaluate the challenges that may hinder their clinical deployment and propose future research directions, bridging the gap between the bench and the bedside.

INTRODUCTION

A blood clot is a mass of blood that has changed from a liquid to a gel-like state. This physiological process is essential for preventing excessive blood loss and facilitating wound healing.[1,2] However, blood clots may form undesirably within blood vessels and lead to ischemia in downstream organs and tissues. The clinical manifestations of intravascular thromboembolism depend on the location and severity of the occlusion. When thromboembolism occurs in an artery, it may trigger immediate symptoms such as severe pain (e.g., peripheral limb ischemia), dull chest pain, cardiac events (e.g., myocardial infarction), paralysis of body parts (e.g., stroke), or even death. By comparison, venous thromboembolism is generally less acute than arterial thromboembolism but can still be life threatening, as thrombi or emboli may travel within the circulatory system to various regions/organs, such as the legs, abdomen, lungs, heart, and brain, obstructing blood flow.

Among the various arterial thromboembolic diseases, ischemic stroke is a global health risk with high mortality rates and one of the most commonly encountered emergencies.[3,4] According to the World Health Organization, strokes affect 15 million people globally, leading to 5 million deaths and leaving another 5 million with permanent disabilities each year. Moreover, strokes are particularly prevalent among the elderly, especially those with hypertension, making it one of the most fatal diseases. The effects of stroke are diverse, ranging from mild limb weakness to permanent paralysis, speech impairment, or even death, which depend on the infarct territories and treatment response.[5] The definitive therapy should ideally be performed within the first few hours after stroke onset to quickly restore cerebral perfusion and minimize neuronal cell death. Previous therapies for the removal of thrombus can be classified into two categories: (1) mechanical thrombectomy, which employs a catheter to extract the occluding blood clot, and (2) thrombolysis, which relies on the diffusion of thrombolytic agents to degrade the blood clot.[6] In recent years, endovascular thrombectomy (EVT) has gained considerable attention due to encouraging outcomes from clinical trials.[7–10] EVT involves using thrombectomy devices, including coil retrievers, aspiration devices, and stent retrievers, to remove the clot under angiographic and fluoroscopic guidance, achieving reperfusion and neurological recovery.[11–13] However, the applicability of EVT is limited by several challenges. First, cerebral large-vessel occlusion (LVO) accounts for 24%–46% of total ischemic strokes,[14] meaning that over half of ischemic strokes may not be treatable with EVT. Second, anatomical and technical challenges may prevent timely reperfusion. For instance, unfavorable aortic arch anatomy in cerebral vessels may hinder the navigation of thrombectomy catheters, resulting in prolonged procedure time. Therefore, the success of EVT substantially depends on the expertise and experience of specialized doctors. For example, many thrombi are located in hard-to-reach regions (e.g., M3/M4 segments of cerebral vascular), where skilled and experienced professionals are needed to manage the situation; otherwise, it may result in device fracture, vessel perforation, or hemorrhage.[15,16] Unfortunately, in many developing countries and underserved rural areas, it is challenging to quickly access large hospitals and experienced doctors. Additionally, distal emboli caused by clot fragmentation after the first pass of thrombectomy may not be retrievable with current thrombectomy systems.

Apart from mechanical thrombectomy, thrombolysis is another efficient method for thrombus treatment using thrombolytic agents such as recombinant tissue plasminogen activators (tPA).[17] tPA is a serine protease found on endothelial cells that can catalyze the conversion of plasminogen (PLG) to plasmin (PLM), which then binds to fibrin and breaks down blood clots to restore blood flow. Thrombolysis is typically conducted via intravenous (i.v.) injection of thrombolytic agents. Large-scale trials of tPA in acute ischemic stroke (AIS) treatment have demonstrated convincing benefits in survival rate and functional status with prompt treatment initiated within 6 h.[18] However, tPA usage is associated with an increased risk of symptomatic intracranial hemorrhages (SIH) due to systemic fibrinolysis, which could be fatal. According to the guidelines for managing patients with AIS published by the American Heart Association Stroke Council in 2007,[19] the recommended dosing regimen of i.v. tPA treatment is 0.9 mg/kg, with a maximum limit of 90 mg per treatment.[20] To date, dose control remains the primary strategy to minimize the risk of SIH associated with tPA administration. Balancing these risks and benefits, tPA is commonly recommended for use within 3–4.5 h of stroke onset.[21,22] Rapid and efficient delivery of tPA to the occlusive site is essential for treating AIS. To improve treatment efficacy and safety, new strategies are urgently required to enhance thrombolysis while reducing the risk of adverse effects.

Recently, with the rapid development of nanomaterials and nanotechnology, miniature robots (MRs) have attracted significant attention and offer a promising new drug-delivery strategy for thrombus treatment.[23–27] Various MRs serve as active carrier building blocks for loading drugs such as tPA to realize highly targeted and controlled release, thereby enhancing local efficacy. Compared to traditional methods, MR-based systems may require smaller drug dosages, thereby substantially reducing the risk of side effects.[28–36] To establish a platform for vascular blockage treatment, three critical aspects should be considered: the rational design principles of MRs, the effective actuation system, and the real-time localization/tracking method. Besides, many challenges still need to be overcome to translate MRs from the bench to the bedside. In this review, we summarize recent progress in vascular blockage treatment based on emerging MR-based techniques. Design principles of MRs from both engineering and clinical perspectives are introduced based on the complex endovascular

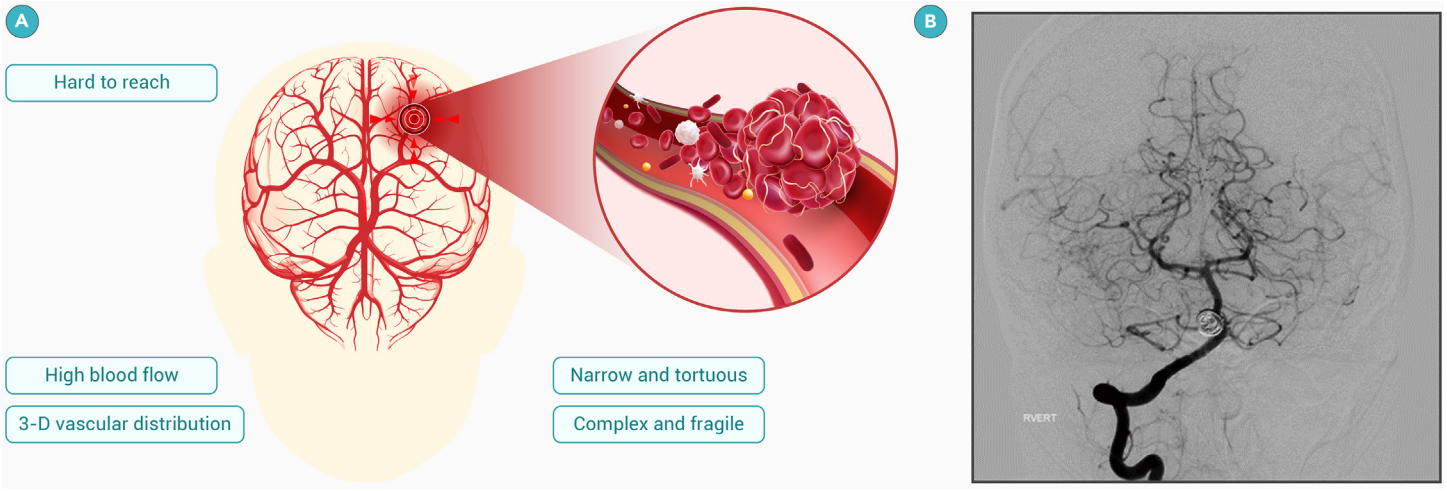

Figure 1. Properties of the cerebral vascular environment (A) Schematic of cerebral blood vessels. (B) Real CT imaging of human cerebral blood vessels.[46] Copyright 2014, The Authors.

environment. Additionally, we discuss existing problems, challenges, and future development directions in this field to further leverage MR-based therapeutic platforms for vascular recanalization across different organs in the human body.

THROMBUS PATHOPHYSIOLOGY AND ENDOVASCULAR ENVIRONMENT

The design of MRs is rooted in the thrombus pathophysiology and the unique characteristics of the endovascular environment. This section provides a basic introduction to both thrombus formation and the specific properties of the endovascular lumen, facilitating the design and development of MRs tailored for thrombus treatment.

Thrombus formation and consequences

Thrombus formation is governed by three interrelated factors, namely endothelial injury, abnormal blood flow, and a hypercoagulable state.[37] Fibrin cross-links with fibronectin to form a fibrin network that stabilizes platelets and red blood cells, resulting in thrombus formation.[38] Thrombi can form *in situ* within blood vessels, and fragments may detach from the embolus and travel through the circulatory system, potentially blocking smaller vessels. The rupture of atherosclerotic plaques and intraplaque hemorrhage is commonly associated with arterial thrombosis, which can lead to severe conditions such as ischemic stroke, acute coronary syndromes, and critical leg ischemia.[39] Venous thromboembolism can occur spontaneously or result from trauma, surgery, or prolonged immobility. Venous thrombosis can arise in any part of the venous system, most commonly in the deep veins of the leg. Ischemic stroke and myocardial infarction share similar features, such as acute onset, a short therapeutic window, and high morbidity and mortality rates, making them among the most perilous life-threatening thrombolytic disorders. Pulmonary embolism is characterized by high short-term mortality and recurrence rates, often presenting with symptoms such as shortness of breath, chest pain, or fainting. Atherothrombosis and deep vein thrombosis typically manifest with mild clinical symptoms but are associated with complications such as swelling, inflammatory disorders, and pulmonary embolism. Among these conditions, ischemic stroke treatment remains a significant clinical challenge due to the fragile nature of brain tissue and the complexities of the endovascular environment; thus, it has been selected as a clinical model for discussion in the following sections.

Endovascular environment

MRs are expected to enter blood vessels and navigate within them for targeted thrombus removal. The design of MRs for endovascular deployment necessitates a comprehensive understanding of the properties of the endovascular environment, such as vascular dimension, shear stress, and flow velocity, to identify the challenges involved. This discussion mainly focuses on the cerebral vascular segment, which represents the most complex and tortuous distribution of blood vessels, posing significant obstacles to clinical stroke treatment. The diameter of blood vessels varies from over 20 mm (e.g., main arteries) to under 10 μm (e.g., capillaries) at different vascular segments.[40–44] For cerebral vessels, the internal carotid artery (ICA) has a relatively large diameter range of 3.5–5.0 mm, while the vascular dimension gradually decreases in branched segments. For example, as the branch number increases from M1 to M4, the diameter of the branches progressively reduces to a range of 1.0–1.5 mm. Furthermore, the vessel diameter can be less than 1 mm in distal brain regions, such as the posterior cingulate, anterior cingulate, parahippocampal gyrus, and temporal gyrus.[40,45] Even more challenging, these narrow vessels often have unfavorable 3D anatomical features, such as sharp turns, as shown in Figures 1A and 1B, making it difficult to remove thrombi via thrombectomy in these intricate regions. In comparison, MRs, benefiting from their small body size, can flexibly navigate through narrow and tortuous cerebral vessels under remote control, thus achieving effective thrombus removal.

However, achieving precise motion control of MRs within cerebral vessels remains a critical issue, primarily due to the high shear pressure associated with strong blood flow. Shear stress, which increases significantly in stenotic vessels, complicates the navigation of MRs, resulting in instability, uncontrollability, and motion failure of MRs. The pulsatile blood flow in arteries varies from 100 to 400 mm/s, whereas venous blood flow is relatively low.[47] Although blood flow slows decrease in the branches, the lowest velocity in capillaries can still be about 100 μm/s, which significantly affects the motion behavior and controllability of MRs.[48] Moreover, with the thrombus formation, the blood vessel may become stenotic, causing shear stress to increase dramatically up to 1,000 dyne/cm^2.[24,49,50] Designing MRs with enhanced propulsion and environmental adaptations is critical for overcoming these forces.[49] For example, $CaCO_3$-based micromachines can generate a large number of bubbles to generate sufficient thrust force against the flow velocity of up to 1.8 mm/s.[51] Navigating the MRs along the blood vessel wall is another effective way to minimize the disturbing effect of high blood flow. Microrobots can maintain controllable movability because the flow velocity and fluid resistance near the boundary conditions are much lower than in the vessel center. Inspired by the leukocyte, researchers confirmed that microrollers could efficiently move against physiologically relevant blood flow (1.2 dyne/cm^2) along the vessel wall.[52] This benefit reduced the demand for large propulsion force, allowing them to better overcome the obstacles posed by dynamic blood flow. Zhang et al. demonstrated active upstream locomotion of magnetic microswarms along the vessel wall with a mean velocity of up to 35 mm/s under real-time ultrasound (US) imaging guidance.[53] More recently, they explored using a balloon catheter to temporally mediate high blood flow, enabling active targeted delivery of therapeutic agents across a wide range of flow velocities. These promising strategies underscored the feasibility of employing MRs to tackle thrombi in cerebral vessels and potentially enhance stroke treatment outcomes.[3]

DESIGN PRINCIPLES OF MRs

To effectively address thrombi within the complex and dynamic endovascular environment, MRs must be engineered to align with the specific requirements

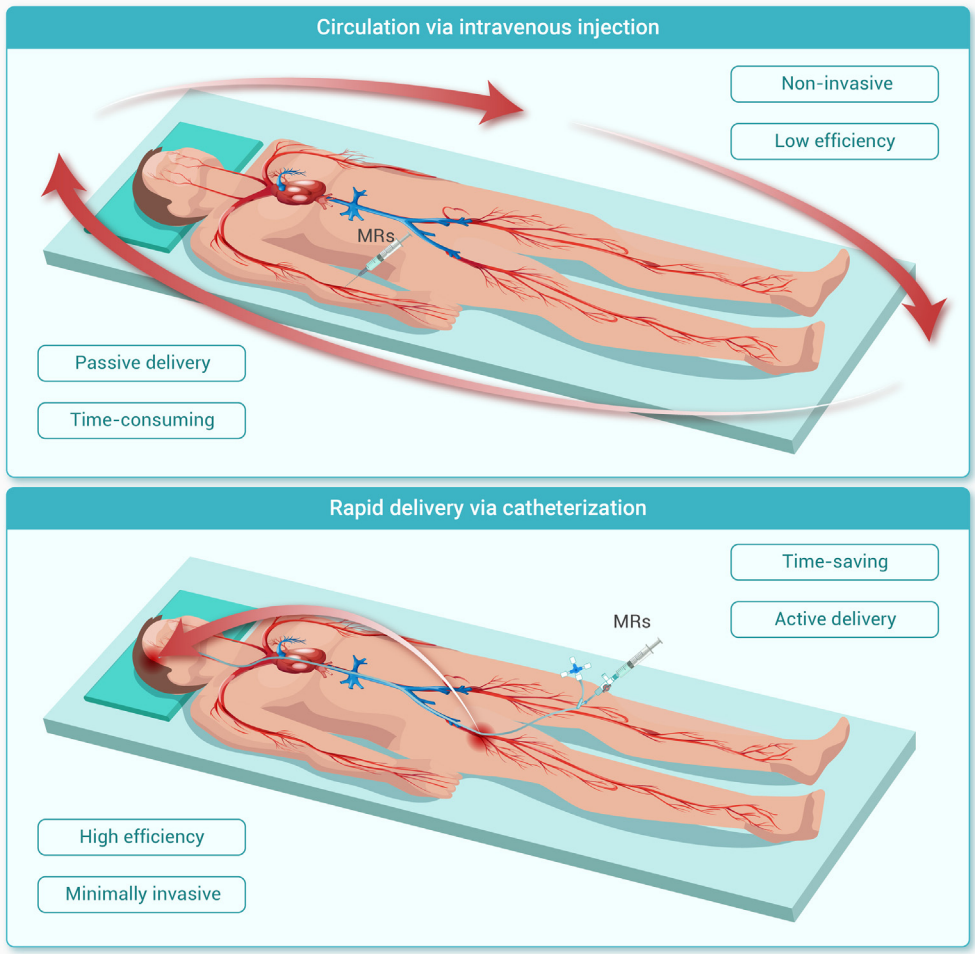

Figure 2. Comparison between direct i.v. injection and catheterization for long-distance delivery of MRs

imposed by real biophysical conditions. The key factors that determine the therapeutic effect of MRs are discussed in the following sections.

Long-distance delivery of MRs

Thrombus treatment, especially for ischemic stroke, is a time-dependent procedure, necessitating the rapid deployment of MRs at a human scale. For long-distance delivery of MRs (e.g., from the patient's leg to the brain), two strategies can be employed, namely i.v. injection and catheterization. I.v. injection of MRs offers advantages such as minimal invasiveness, quick administration, and operational simplicity. However, its lack of precision may lead to treatment failure.[54,55] This approach relies on the bloodstream for transporting the MRs, which is passive and inefficient, causing undesired accumulation in non-targeted organs. Additionally, some MRs may be cleared by metabolism and cellular internalization during circulation, further reducing their accessibility to the clotting region. Although specific modifications to MRs could improve their targeting ability, their efficiency remains low. Passive diffusion determines the transportation of MRs once the blood vessel is completely occluded by the thrombus, which makes it difficult for MRs to reach the thrombus with a nearly stagnant bloodstream, resulting in prolonged treatment duration.[56,57] In comparison, combining MRs with catheter deployment is a promising strategy for effective and safe long-distance delivery.[58] Catheterization allows the rapid and precise delivery of MRs to specific locations within the body (e.g., from the patient's leg to the brain, for stroke treatment; Figure 2). Before catheterization, angiography is conducted to verify the location of the thrombus, and MRs are pre-deployed inside the catheter. Then, an imaging-guided intervention procedure can be performed by surgical clinicians, allowing the catheter to rapidly access the targeted site near the thrombus. Subsequently, MRs are released from the catheter and actuated toward the thrombus with a short distance for highly precise treatment. Throughout the delivery process, the catheter serves as a protective conduit, significantly minimizing the impact of dynamic blood flow on the MRs and avoiding unnecessary biodistribution and accumulation in non-targeted locations, which ensures high delivery efficiency. Moreover, the catheterization process is guided by clinical imaging modalities, enhancing the accuracy of the delivery process and benefiting localized therapy. Therefore, the precisely controlled intervention process via catheterization is suitable for the long-distance deployment of MRs, despite some disadvantages such as minimal invasiveness and the need for proficiency in surgical skills.

Actuation of MRs

Various power sources have been explored for the actuation of MRs, including light, electricity, US, and magnetic fields. Selecting the appropriate propulsion mechanism is crucial for achieving active and dexterous motion of MRs in the complex and dynamic endovascular system.[51,53,59–65] On the one hand, the propulsion force should be sufficient for MRs to overcome the drag force imposed by blood flow, especially in the cerebral artery, where flow velocity can vary significantly; on the other hand, the actuation methods must be compatible with clinical imaging tools, such as US imaging, X-ray imaging, and MRI, to enable real-time navigation feedback for safe and effective intervention procedures. Chemically driven MRs have demonstrated the potential for active propulsion within blood vessels by harvesting energy from the surrounding environment.[66,67] These MRs typically feature a Janus structure, allowing asymmetric reactions to achieve either self-diffusiophoresis, induced by an osmotic gradient from the high molecular concentration of products on the catalyst side,[68] or self-electrophoresis, triggered by electroosmotic flow due to electron migration from the catalyst to the metal side.[69] However, both types of chemically driven MRs are highly sensitive to ion concentrations, resulting in low propulsion efficiency or even propulsion failure in the high-ion environment of blood.[70] To mitigate this limitation, bubble-driven MRs have been explored, utilizing the driving force generated by bubble formation and detachment for propulsion.[51] However, their non-directional motion deteriorates controllability in vascular environments, and bubble generation poses safety concerns due to potential occlusions. Similar to chemical propulsion, light-driven MRs can achieve active motion via self-diffusiophoresis and self-electrophoresis, while light serves as the energy source instead of chemical fuels.[71,72] Near-infrared (NIR)-triggered self-thermophoresis, driven by thermal gradients, employs photothermal conversion materials (e.g., Au and polydopamine) to construct MRs.[73,74] However, limited tissue penetration remains a significant obstacle for light-driven MRs, particularly for thrombus treatment in intracranial areas shielded by the skull.[75] Acoustic-driven MRs, utilizing non-invasive and versatile acoustic fields as power sources, can achieve precise and maneuverable actuation in endovascular environments.[62,76,77] These MRs are propelled by two types of acoustic wave-induced forces: acoustic streaming and acoustic radiation (lower left part of Figure 3).[78] Acoustic streaming results from local oscillation at solid-liquid or air-liquid boundaries, as acoustic waves are absorbed while transitioning from oscillating solids or gases to the liquid medium. MRs designed with oscillating units, such as asymmetric structures or cavities trapping with air bubbles, generate propulsion forces through surface streaming stresses. Acoustic radiation force, exerted on MRs suspended in a liquid medium, consists of gradient and scattering force. The dominance of these two forces depends on the wavelength (λ) of acoustic waves and the dimension (d) of the MRs. Acoustic-driven MRs hold promise for thrombus treatment, particularly when combined with synergistic sonodynamic therapy utilizing acoustic forces in soft tissues; however, the acoustic shadowing effect makes

them hard to adopt in regions with bones (e.g., the intracranial area), complicating control over the MRs. Biohybrid-driven MRs, inspired by engineered living organisms such as algae, paramecia, and sperm, represent an emerging drug-delivery platform for vascular disease treatments (e.g., pneumonia and cancer).[64,79] As shown in the lower right part of Figure 3, the flagellar beating of sperm generates propulsion by pushing fluid backward, while tangential drag friction is lower than normal drag.[80] However, the random motion of biohybrid-driven MRs leads to compromised controllability. This issue could potentially be addressed by incorporating magnetic-responsive materials for external guidance, and the application of biohybrid-driven MRs for occlusion therapy remains an area that requires further exploration.

Precise remote actuation of MRs can be achieved through magnetic manipulation, which features high safety, deep tissue penetration, and reliable intracranial operation for stroke treatment.[81–83] Applied with a magnetic field, MRs are subjected to magnetic torque and/or magnetic gradient forces.[84] As shown in the equations in the upper right part of Figure 3, the force exerted on a magnetic object is zero under a uniform magnetic field. Therefore, to enable continuous motion of MRs, the magnetic field must exhibit spatial and/or temporal changes. Torque-driven MRs typically show helical or helical-like structures, which offer superior locomotion performance through a spiral propulsion mode when subjected to external magnetic fields.[85,86] With the direction of a uniform magnetic field changing, the magnetized MR is deflected by magnetic torque due to the misalignment between its magnetic dipole moment and the field direction. Consequently, when a uniform magnetic field rotates around the long axis of the helical MR, the robot rotates continuously, allowing for directional motion along the axis. By contrast, specialized structures are not required for gradient-driven MRs, as gradient magnetic fields inherently possess spatial changes.[87,88] These MRs can achieve continuous movement as long as the magnetic force exceeds the frictional and/or drag forces within the fluid medium. Beyond single MRs, researchers have also explored applying magnetic fields to induce swarming behavior among numerous building blocks.[83,89–91] Medium-induced swarms can form under a rotating magnetic field, while magnetic field-induced swarms arise under oscillating fields. These microswarms offer advantages such as adaptive environmental transformation, batch delivery capability, and enhanced imaging contrast, making them promising candidates for precise therapy within the endovascular system. Given the complex structure and dynamic environment of the cerebral system, achieving precise 3D navigation of magnetically driven MRs under high-blood-flow conditions is challenging. Several strategies can potentially be adopted to address this issue: (1) proper structure design of MRs is required for efficient locomotion, e.g., adopting helical structure for torque-driven MRs; (2) using materials endowed with high magnetization, such as Fe, Fe_3O_4, FePt, Ni, to construct the MRs, thus generating sufficient magnetic forces to overcome bloodstream drag; (3) designing the magnetic actuation system with high magnetic field strength to exert greater force outputs on the MRs; (4) employing navigation approaches that allow MRs locomoting near the vessel wall, where the blood flow is much lower than the center area; (5) implementing surgical techniques to reduce or halt the blood flow, e.g., via balloon-catheter intervention, enabling flexible locomotion of MRs; (6) integrating the magnetic actuation system with clinical imaging tools, e.g., fluoroscopy imaging, is necessary for real-time tracking and navigation of MRs, ensuring safe and effective manipulation.[63] Taken together, magnetic-driven MRs show great potential for thrombus removal in tiny and tortuous vascular sites, especially in cerebral regions, with reliable and feasible actuation and navigation strategies.

Imaging of MRs

Real-time imaging and tracking of MRs can provide timely feedback to operators, ensuring safe, accurate, and reliable control strategies.[92–94] Various techniques have been used for the localization of MRs, as shown in Figure 4, including fluorescence imaging (FI),[99,100] photoacoustic computed tomography (PACT) imaging,[96] laser speckle contrast imaging (LSCI),[97] US imaging,[101,102] MRI,[103–105] positron emission tomography (PET),[106] X-ray fluoroscopy imaging,[3] and photoacoustic imaging (PAI).[107] These imaging modalities hold different properties in terms of penetration ability, spatial resolution, temporal resolution, and so on; thus, adopting proper tools for localization of MRs based on specific endovascular environments is also critical for accurate navigation.

In an ideal scenario, medical imaging modalities for tracking MRs should offer high spatiotemporal resolution and compatibility with actuation and navigation systems. Detailed information on vascular distribution and structure should be provided by imaging modalities, which is essential for the path planning of MRs and ensuring successful access to the targeted site. Optical-based imaging tools show high biosafety and relatively low cost, which have been adopted for imaging of MRs with high spatial (tens of micrometers) and temporal (seconds to minutes) resolutions (Figure 4G).[108,109] The working principles of optical imaging modalities for tracking MRs can be categorized into fluorescence-based techniques and reflection-based techniques. Fluorescence imaging relies on light emitted from MRs upon excitation with incident light (Figure 4A), whereas reflection-based imaging depends on light reflected from the MRs. Wang et al. demonstrated the use of LSCI to track and navigate an Fe_3O_4-based microswarm in the vascular environment *in vivo*, showing advantages including real-time feedback, a large imaging field, and high spatial resolution (Figure 4C).[97] However, limited tissue penetration of light remains the primary obstacle for imaging of MRs in blood vessels located in deep tissues, particularly within cerebral vasculature. Although optical-based imaging tools can hardly be employed in a clinical scenario, the exploration of the thrombolysis process in subcutaneous tissues (e.g., pig ear and rat femoral vein) is feasible, enabling *in vivo* thrombolysis performance evaluation of MRs and benefiting the design and optimization of MRs. In comparison, US imaging has been widely used in clinical settings due to its non-invasiveness, relatively high spatiotemporal resolution, and deep penetration capabilities in soft tissues, making it suitable for real-time tracking and localization of MRs in blood vessels.[110] Both B-mode and Doppler-mode US imaging have been investigated for imaging and tracking MRs. For example, real-time tracking of a helical robot was realized by US feedback (B mode) with a spatial resolution of submillimeter for targeted disruption of the blood clot. Except for single MRs, Wang et al. demonstrated the application of US imaging to track microswarms in complex and dynamic vascular environments with multi-viewing configurations, providing insights into blood-flow conditions under Doppler mode.[53] The imaging signals generated by B mode and Doppler mode depend on the echogenicity (the property of backscattering US waves) and the moving velocity of the objects, respectively. Despite its potential for real-time imaging of MRs in biological environments, US imaging faces challenges related to long-distance tracking and navigation of MRs within the vascular system. On the one hand, the restricted acoustic window of US imaging requires continuous manipulation of the US probe for long-distance tracking, which may cause signal loss or even imaging failure. On the other hand, the acoustic shadowing effect (strong acoustic wave absorption by bones) limits its deployment in intracranial blood vessels.[111] Moreover, body movements and breathing could generate strong noisy signals, attenuating the imaging quality. Recently, PAI combining the high spatial resolution of light with the deep penetration ability of US has emerged as a promising tool for the localization of MRs. Sitti et al. reported real-time optoacoustic tracking of individual microrobots with a diameter of 5 μm in the mouse brain vasculature.[96] Nonetheless, due to the limitations of light, the tissue penetration depth is restricted to only a few centimeters, making it challenging to adopt this method for tracking MRs in large animals or humans.

MRI can provide whole-body imaging due to its high penetration depth, which is clinically used to acquire 3D anatomical images of soft tissues and organs for diagnosis. Magnetic particles are commonly used as imaging contrast agents due to their high relaxivity. Previous studies have demonstrated the use of MRI for tracking both single and swarming magnetic MRs across various scales.[112] A unique advantage of MRI is its capacity for simultaneous actuation and imaging of MRs via the strong magnetic field generated by the gradient coils. However, the trade-off between spatial and temporal resolution leads to prolonged imaging processing times, which complicates the real-time tracking of MRs. Ionizing radiation-based imaging modalities, such as CT, PET, and fluoroscopy, offer advantages of high spatial resolution and deep tissue penetration, which are widely adopted in clinical settings.[113–115] However, real-time tracking of MRs is difficult to achieve by CT imaging due to its low temporal resolution, while PET imaging cannot provide morphological and anatomical features of the blood vessel, attenuating the precise targeting ability of MRs in complex environments. Among these imaging modalities, fluoroscopy imaging is commonly used for guiding surgical interventions in stroke patients. Its high temporal and spatial resolution makes it suitable for imaging and localizing MRs in endovascular lumens, particularly within cerebral vasculature. More importantly, its compatibility with actuation systems facilitates effective and accurate control of MRs. Sukho et al. demonstrated using the microrobot to treat arterial thromboembolism in

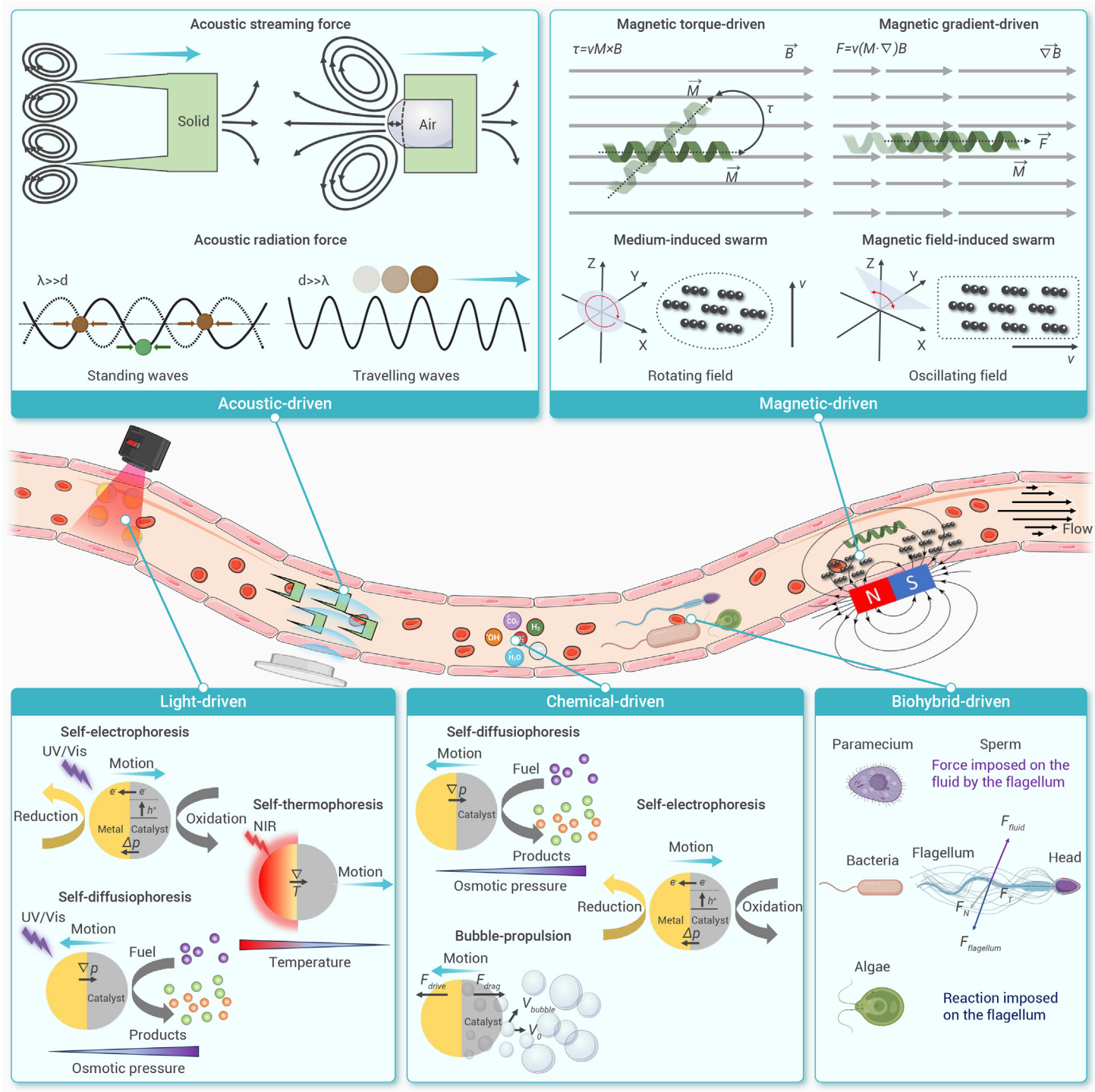

Figure 3. Actuation mechanism of various MRs, including light-driven, magnetic-driven, acoustic-driven, chemical-driven, and biohybrid-driven MRs ∇p refers to the pressure gradient; ∇T refers to the temperature gradient; λ refers to the wavelength of acoustic waves; d refers to the dimension of the MRs; F_{drive} refers to the driving force; F_{drag} refers to the viscous drag force; V_{bubble} refers to the bubble's velocity; V_0 is the velocity of the initial horizontal component of the detached bubble; F_N refers to the normal drag force perpendicular to the tail surface; F_T refers to the tangential drag force parallel to the tail surface; v, M, B, τ, and F denote the volume and magnetization of the MR, magnetic flux of the external magnetic field, magnetic torque, and magnetic gradient force, respectively. Part of the schematic was created using BioRender.com.

a pig with real-time guidance by a biplane X-ray imaging platform.[116] Similarly, our group reported employing tPA-modified nanorobots for targeted recanalization in a rabbit model with fluoroscopy imaging.[3] These examples highlight the great potential of using fluoroscopy to achieve real-time tracking and navigation of MRs tailored for ischemic stroke treatment. To enhance the imaging contrast of MRs under fluoroscopy, incorporating high-atomic-number elements, such as Au, Fe, Ti, and Ta, into MRs is an effective approach that increases X-ray absorption.[112] Additionally, inducing the swarming behavior of MRs can further improve imaging contrast due to the increased area density of locally accumulated building blocks. The fluoroscopy imaging-guided approach allows for real-time visualization and navigation of MRs, ensuring the precise deployment of MRs within the intricate network of the cerebral system.

Biosafety of MRs

MRs are specifically engineered to navigate in blood vessels and remove thrombi at targeted sites, while improper design and administration may pose biosafety risks (e.g., vascular damage, toxicity, and undesired immune response).[24,47] Therefore, selecting materials with inherent biocompatibility and non-toxicity is crucial when designing MRs for thrombus treatment. Preferred biocompatible materials consisting of polymers like polylactic-co-glycolic

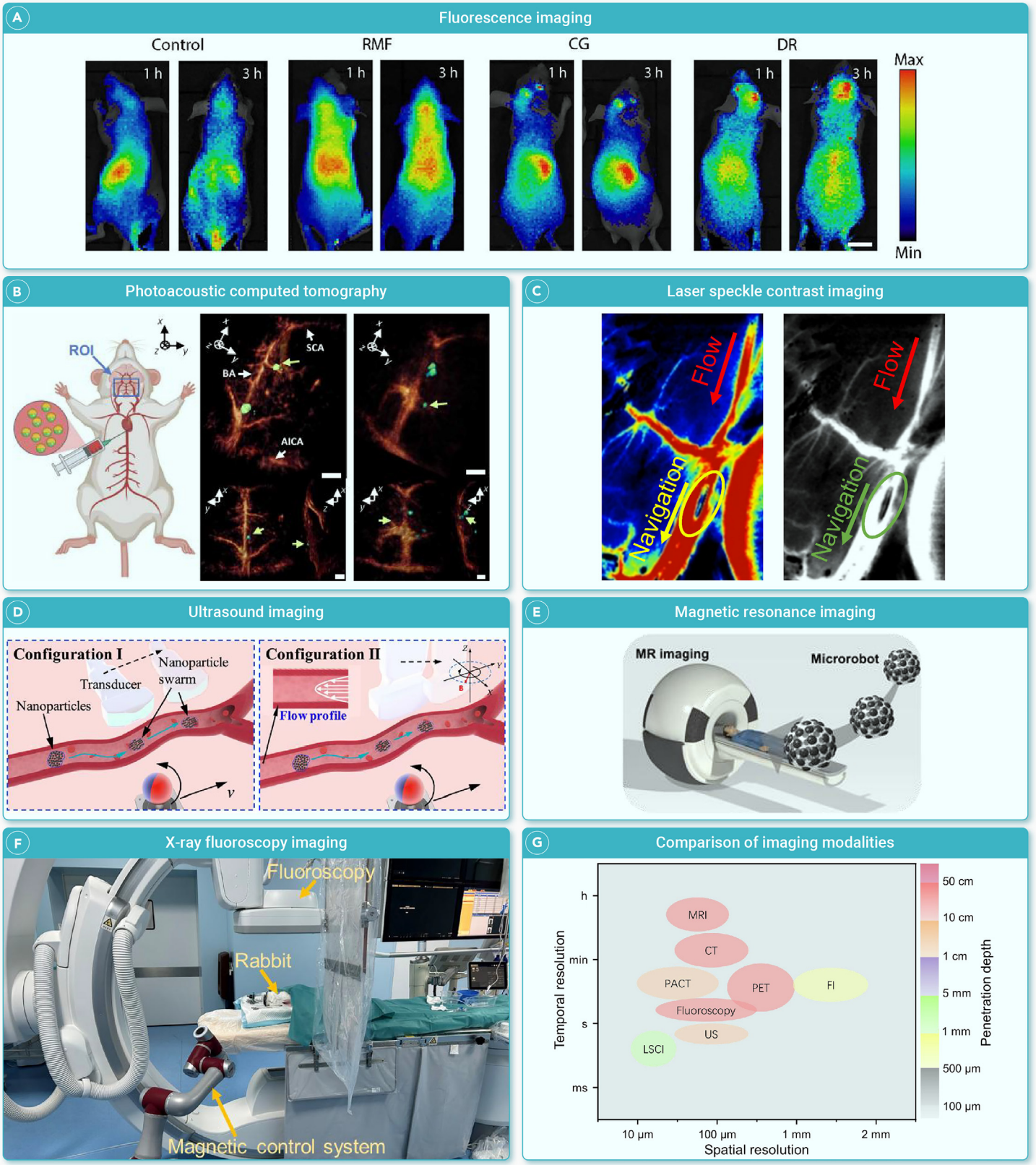

Figure 4. Examples of common imaging modalities used for imaging and localization of MRs (A–F) Various imaging tools used for MRs, including (A) fluorescence imaging (FI),[95] Copyright 2021, The Authors; (B) photoacoustic computed tomography (PACT) imaging,[96] Copyright 2022, The Authors; (C) laser speckle contrast imaging (LSCI),[97] Copyright 2024, The Authors; (D) ultrasound (US) imaging,[53] Copyright 2021, The Authors; (E) magnetic resonance imaging (MRI),[98] Copyright 2022, The Authors; and (F) X-ray fluoroscopy imaging.[3] Copyright 2024, The Authors. (G) Comparison of imaging modalities in terms of spatial resolution, temporal resolution, and penetration depth.

acid (PLGA),[117] polylactic acid (PLA),[118] and polycaprolactone (PCL)[119]; biomaterials like alginate,[120] chitosan,[121] and cell membranes[122]; metals like Mg,[123] Ti,[124] and Au[125]; and oxide materials like TiO_2,[126] Fe_3O_4,[127] and MnO_2[128] have been adopted for the development of MRs. Furthermore, altering the surface properties of the MRs is an important approach to minimize undesired interactions. Common surface modifications such as polyethylene glycol (PEG) coatings,

cell membrane camouflage, or bioinspired designs have been applied to reduce protein adsorption, enhance circulation time, and prevent thrombosis or hemolysis.[129,130]

Following the removal of the thrombus, post-treatment of MRs becomes imperative. Passive clearance mechanisms represent a basic approach for ensuring the safe elimination of MRs, typically those with dimensions below 10 nm. These mechanisms capitalize on natural physiological processes to metabolize or expel the MRs without requiring external interventions. Endocytosis allows cells, particularly macrophages and other phagocytic cells, to internalize the MRs, followed by intracellular degradation via lysosomal activity or enzymatic breakdown. This pathway ensures that the MRs are processed and removed in a biocompatible manner, minimizing potential inflammatory or immune responses. Additionally, urinary excretion relies on the renal filtration system to eliminate MRs through the kidneys, provided their size and surface properties allow for efficient glomerular filtration. The effect of these passive clearance pathways is highly dependent on the physicochemical properties of the MRs, including their size, shape, material composition, and so on. These factors should be meticulously optimized during the design phase to align with the body's clearance thresholds.

In scenarios where biodegradation is impractical, retrieval-focused designs become necessary. For instance, modular microrobots with detachable therapeutic components have been developed to deliver payloads *in situ* while allowing the magnetic navigation module to be retrieved safely after treatment.[131] As the magnetic components are non-degradable, such designs ensure that therapeutic tasks are executed efficiently with degradable processes while minimizing the risks of magnetic materials accumulating in the therapeutic region. Active retrieval strategies are particularly vital in the cerebral vasculature to prevent long-term complications. Magnetic actuation systems integrated with interventional tools like catheters have been used to guide MRs back to accessible locations for removal. For example, balloon-catheter-mediated magnetic-driven MRs have been successfully demonstrated for thrombolysis in submillimeter-scale vessels, ensuring precise targeting and retrieval under imaging guidance.[3] The "wait-and-capture" strategy, leveraging blood circulation and intravascular magnetic catheters, offers an effective solution for capturing magnetic MRs post treatment, reducing the risk of their dispersion in non-target areas. For example, a magnetic stent with trapping channels has been designed to capture MRs near stented regions, allowing safe extraction in a minimally invasive manner.[132] During the retrieval process, imaging modalities play a crucial role in real-time monitoring, which guarantees precise navigation and retrieval of MRs in delicate environments.

Physical and surface properties of MRs

In addition to biological safety, several critical factors must be considered when developing MRs to ensure their feasibility for clinical applications in intravascular environments. One key consideration is size, as MRs should be small enough to navigate through the intricate and narrow vascular network without causing blockages, especially in tiny branches like arterioles and capillaries. Moreover, the dimensional design must balance functionality, as excessively small MRs may face difficulties related to controllability, propulsion efficiency, and poor capability of therapeutic payloads.[58] Apart from size, the mechanical properties of MRs are also important for their intravascular applications. Unlike traditional biomedical devices, which may require high stiffness for structural integrity, MRs deployed in vascular environments prefer lower stiffness to minimize the risk of vascular or tissue damage. High stiffness can result in mechanical trauma to the delicate endothelial lining of blood vessels. Materials with lower elastic moduli, such as hydrogels or soft elastomers, are therefore prioritized.[133] Furthermore, the mechanical adaptability of MRs, such as the ability to deform reversibly under external forces, can enhance their ability to navigate through narrow or highly curved vessels without causing obstruction or injury.[134] Recent advances in stimuli-responsive materials, such as shape-memory polymers or magnetoelastic composites, have enabled the development of MRs with dynamic mechanical properties that adjust in response to environmental conditions, thereby further improving their safety and functionality in vascular applications.[135,136]

The surface properties of MRs are equally crucial, as their interaction with the blood environment determines their circulation time, distribution, and therapeutic efficacy. One prominent challenge is the formation of a protein corona, which occurs when blood proteins adsorb onto MRs through dynamic and competitive interactions. This protein corona can alter the physicochemical properties of MRs, such as their size, surface charge, and hydrophobicity, potentially leading to compromised targeting specificity, impaired propulsion, or accelerated clearance by the immune system.[137–139] The composition of the protein corona depends on factors such as the MR's surface chemistry, size, and the local blood protein profile. To avoid protein corona formation on MRs, one could use hydrophilic coatings (e.g., PEGylation) to create a steric barrier that prevents protein adsorption, or one could alter the surface charge of MRs to reduce protein binding.[140] Additionally, pre-coating MRs with specific proteins can create a "stealth" effect, reducing direct exposure to undesired proteins.[141] Lastly, optimizing the route of administration can minimize protein exposure, e.g., adopting a catheter for long-distance delivery of MRs instead of whole-body circulation, reducing the odds of protein corona formation in the blood environment. By combining these strategies, it is feasible to significantly reduce protein corona formation, thereby enhancing the stability and effectiveness of MRs for endovascular applications.

LABORATORY STUDY

Here, we summarize the MRs designed for thrombus treatment in Table 1, including mechanisms, thrombus conditions, related devices, and other relevant factors, which provides a foundational overview of the current state-of-the-art in thrombus therapy.

Millimeter-scale robots

For thrombus treatment, MRs with relatively large sizes offer distinct advantages, such as powerful thrust, high imaging contrast, and reliable motion control. Nelson et al.[159] first proposed a wirelessly magnetic-driven robot to treat retinal vein occlusion (RVO). Direct injection of tPA at the occlusion site requires exceptional surgical skills, and improper operation may damage the delicate and fragile retinal vessels. In contrast, the designed robot enables minimally invasive treatment of RVO with prolonged drug release via magnetic-controlled injection. Generally, two therapeutic modes have been adopted for millimeter-scale robots specifically tailored for thrombus treatment. In mode 1, force output generated by millimeter-scale robots enables direct mechanical disruption of the thrombus. To achieve this, millimeter-scale robots are commonly designed with helical shapes that enhance force output by rotational motion,[88,160–162] allowing effective mechanical grinding of blood clots. Leclerc et al.[148] demonstrated a helical magnetic machine that achieved a high thrombus removal rate through efficient mechanical abrasion; a blood clot with a 3-mm diameter and 5-mm length was cleared after 161 s (Figure 5A). To further improve thrombus removal efficiency, mode 2 combining mechanical disruption and drug degradation facilitates an accelerated recanalization process. As shown in Figure 5B, a magnetic-driven machine with a helical thread was developed, which was equipped with a chamber for drug loading to enable both mechanical and chemical disruption of the thrombus. Due to their small size, MRs can access hard-to-reach areas to clear thrombus, while precise motion control within the 3D blood vessel network is required. Therefore, a reliable and effective 3D navigation system is essential for achieving targeted therapy.[164,165] Despite significant progress in the use of millimeter-scale robots for thrombus treatment, several challenges still limit their clinical deployment. Safety concerns arise when these robots lose control, potentially causing damage to fragile vessels or becoming lodged, resulting in occlusion. Mechanical interactions may generate detached blood clot debris, which travels downstream, leading to unpredictable clotting in distal vessels. In summary, millimeter-scale robots can be precisely and wirelessly manipulated to clear blood clots; however, the aforementioned challenges must be addressed before real clinical deployment.

Micro/nanometer-scale robots

Compared to millimeter-scale robots, micro/nano-scale robots possess a unique advantage in navigating narrow and tortuous vasculature, particularly in cerebral vessels. Additionally, their versatile and specific functionalization allows for effective drug delivery and stimulus-responsive behavior, benefiting the thrombolysis process. Cheng et al.[149] developed nickel-based micromachines to accelerate tPA-mediated thrombolysis. The rotation motion of nickel rods under a magnetic field promoted drug diffusion through hydrodynamic convection, thereby accelerating the thrombolysis process (Figure 6A). Besides magnetic fields, light can also be harnessed to power MRs for thrombus removal by

Table 1. Summary of typical MRs for thrombus treatment

		Thrombus condition							
Robot	**Mechanism**	**Source**	**Formation**	**Environment**	**Actuation**	**Imaging**	**Efficiency**	**Property**	**Reference**
Helical robot (300 μm in diameter)	mechanical ablation	human blood	incubated in the vacutainer at 37°C for 1 h	in the PVC tube filled with PBS	magnetic	N/A	reduced by ~50% in 36 min	rapid mechanical removal, powerful penetrating ability	Hosney et al.[142]
μ-Vibrator (20 mm in length)	mechanical ablation	rat blood	uncertain	in the silicone tube filled with physiological-saline	magnetoelastic	N/A	recanalization in 1 h	greater force output, high clot-cleaning efficiency	Xue et al.[143]
Bullet-like robot (2 mm in diameter, 15 mm in length)	mechanical ablation	porcine blood	thrombin and vitamin K were added to the collected blood, then incubated at room temperature for 30 min	in the external iliac artery of pigs	magnetic	X-ray imaging	penetrated in about 40.2 s (SD ±15.11)	stable locomotion, real-time imaging, powerful penetrating ability	Jeong et al.[116]
Helical robot (364 μm in diameter, 4 mm in length)	mechanical ablation	human blood	incubated in the vacutainer at 37°C for 1 h	in the catheter with a flow rate of 10 mL/h	magnetic	N/A	−0.885 mm^3/min	high removal rate compared with chemical lysis	Khalil et al.[144]
Drilling actuator (3 mm in diameter, 9 mm in length)	mechanical ablation	porcine blood	incubated at 80°C for 1h and cooled to 3°C	in a 3D vascular phantom filled with water	magnetic	N/A	penetrated in ~10 s	precise 3D navigation, rapid recanalization	Lee et al.[145]
Helical robot (364 μm in diameter, 4 mm in length)	mechanical ablation	human blood	incubated in the vacutainer at 37°C for 1 h	in the catheter with a flow rate of 10 mL/h (saline) at 25°C	magnetic	US imaging	−0.614 ± 0.303 mm^3/min	real-time tracking, high removal rate	Khalil et al.[146]
Helical robot (1 mm in diameter, 5 mm in length)	mechanical ablation	human blood	incubated in the vacutainer at 37°C for 1 h	in the catheter with a flow rate of 10 mL/h (PBS)	magnetic	US imaging	0.67 ± 0.47 mm^3/min	real-time tracking and imaging, high removal rate	Khalil et al.[147]
Helical swimmer (2.5 mm in diameter, 6 mm in length)	mechanical ablation	human blood	incubated in polydimethylsiloxane (PDMS) tube at 37°C for 5 min	in a PDMS tube filled with PBS at 37°C	magnetic	N/A	12.3 mm^3/min	precise 3D navigation, faster thrombus removal	Leclerc et al.[148]
Helical robot (2.15 mm in diameter, 7.30 in mm length)	mechanical ablation with chemical lysis	porcine blood	1 mL of blood mixed with 20 μL $CaCl_2$ solution (0.5 mol/L)	in silicone tubes filled with porcine blood	magnetic	US imaging	recanalization after 12.33 ± 2.52 min	autonomous navigation, imaging-guided therapy	Wang et al.[63]
Ni nanorod (~1.5 μm in length)	chemical lysis	rat blood	treated by a strip of filter paper soaked with 20% $FeCl_3$ solution for 5 min	in the right femoral vessel of rats	magnetic	N/A	recanalization after 24 h	enhanced drug diffusion	Cheng et al.[149]
Fe_3O_4 nanorod (~1.5 μm in length)	chemo-mechanical lysis	rat blood	mixed 0.4 mL of arterial blood with 80 μL of thrombin (50 U/mL) and 8 μL of calcium chloride solution (1 M)	in a PE 50 catheter filled with saline	magnetic	N/A	decreased by 70% in 60 min	low drug dose, effective drug delivery	Hu et al.[150]
Microwheel (2–10 μm in length)	chemo-mechanical lysis	normal pooled plasma	platelets and fibrin accumulate in the injury channel, forming an occlusive thrombus in ~5 min	in a PDMS channel with 2% BSA in HBS	magnetic	N/A	penetrated the clot in 5 min	enhanced penetration in clots, faster fibrinolysis	Tasci et al.[151]
Microrod (1.3 ± 0.2 μm in length)	chemo-mechanical lysis	rat blood	treated by a strip of filter paper soaked with 10% $FeCl_3$ solution for 1 min	in the distal middle cerebral artery of rats	magnetic	N/A	recanalization in 25 min (for stroke)	enhanced drug transport, rapid recanalization	Hu et al.[152]

(*Continued on next page*)

Table 1. *Continued*

Robot	Mechanism	Thrombus condition			Actuation	Imaging	Efficiency	Property	Reference
		Source	Formation	Environment					
Janus rod-shaped micromotors (~900 nm in width and ~ 1.3 μm in length)	ultrasonication	rat blood	treated by a strip of filter paper soaked with 10% $FeCl_3$ solution for 10 min	the lower limb of the rat	US	N/A	recanalization after 24 h	enhanced thrombus penetration without using any thrombolytic agents	Cao et al.[153]
Microswarm (400 nm in diameter for a single particle)	chemical lysis	porcine blood	1 mL of blood mixed with 20 μL $CaCl_2$ solution (0.5 mol/L)	PDMS channel filled with PBS	magnetic	US imaging	−0.1725 ± 0.0612 mm^3/min	enhanced thrombolysis by microswarm-induced fluid convection, imaging-guided therapy	Wang et al.[154]
Microswarm (156 ± 13.9 nm in diameter for a single particle)	chemical lysis	rabbit blood	100 μL of blood mixed with 10 μL of thrombin (Solarbio, 1,000 U mL^{-1})	in the common carotid artery of the rabbit	magnetic	US imaging	after 90 min, the average thrombolysis length was 0.47 ± 0.05 mm	enhanced thrombolysis by mass transportation, US imaging-guided navigation	Wang et al.[155]
Microswarm (156 ± 13.9 nm in diameter for a single particle)	chemo-mechanical lysis	rabbit blood	the autologous whole blood (~0.1 mL) mixed with thrombin of 100 units	in the common carotid artery of the rabbit	magnetic	US imaging	it takes ~19 min to remove the clot (diameter 1.42 mm, height 4.20 mm)	fast thrombolysis with low drug dosage *in vivo*, a synergy of enzymatic effect and swarming-triggered fluid force	Tang et al.[156]
Microcapsule motors (2 μm in length and 1 μm in diameter)	chemical lysis	rat blood	a filter paper soaked with $FeCl_3$ solution (10%) was placed on the surface of a vein for 5 min	lower limb vessels of the rat	light	N/A	the blood perfusion rate recovered to about 90.5% after 30 min	extended terminal half-life of drug, enhanced penetration in thrombus	Xie et al.[157]
Biomotor (~10 μm in diameter)	chemical lysis	rat blood	filter paper soaked in 10% $FeCl_3$ solution was pasted onto the surface of the carotid artery bypass vessel of the mice for 5 min	the carotid artery of the rat	chemical	N/A	completed thrombolysis within ~30 min	reduced hemorrhagic side effects, promoted thrombolysis, and inhibited re-thrombosis	Zheng et al.[56]
Magnetic nanorobot (760 nm in diameter)	chemo-mechanical lysis	rat blood	filter paper soaked in 10% $FeCl_3$ solution was pasted onto the surface of the femoral vein of the mice for 90 with an extended 5 min for thrombus formation	the femoral vein of the mice	magnetic	US imaging	it exhibited an obvious blood flow signal after 4 h	synergistic thrombolysis by chemo-mechanical lysis, low hemolysis, anti-bioadhesion, and self-anticoagulation	Yang et al.[158]
Microswarm (~300 nm in diameter)	chemo-mechanical lysis with hydrodynamic convection	rabbit blood	1 mL of blood mixed with 20 μL of $CaCl_2$ solution (0.5 mol/L) with incubation of 20 min	the carotid artery of the rabbit	magnetic	fluoroscopy imaging	recanalization within 2 h	better thrombolysis effect, fast delivery, safe retrieval, and clinical imaging-guided therapy	Wang et al.[3]

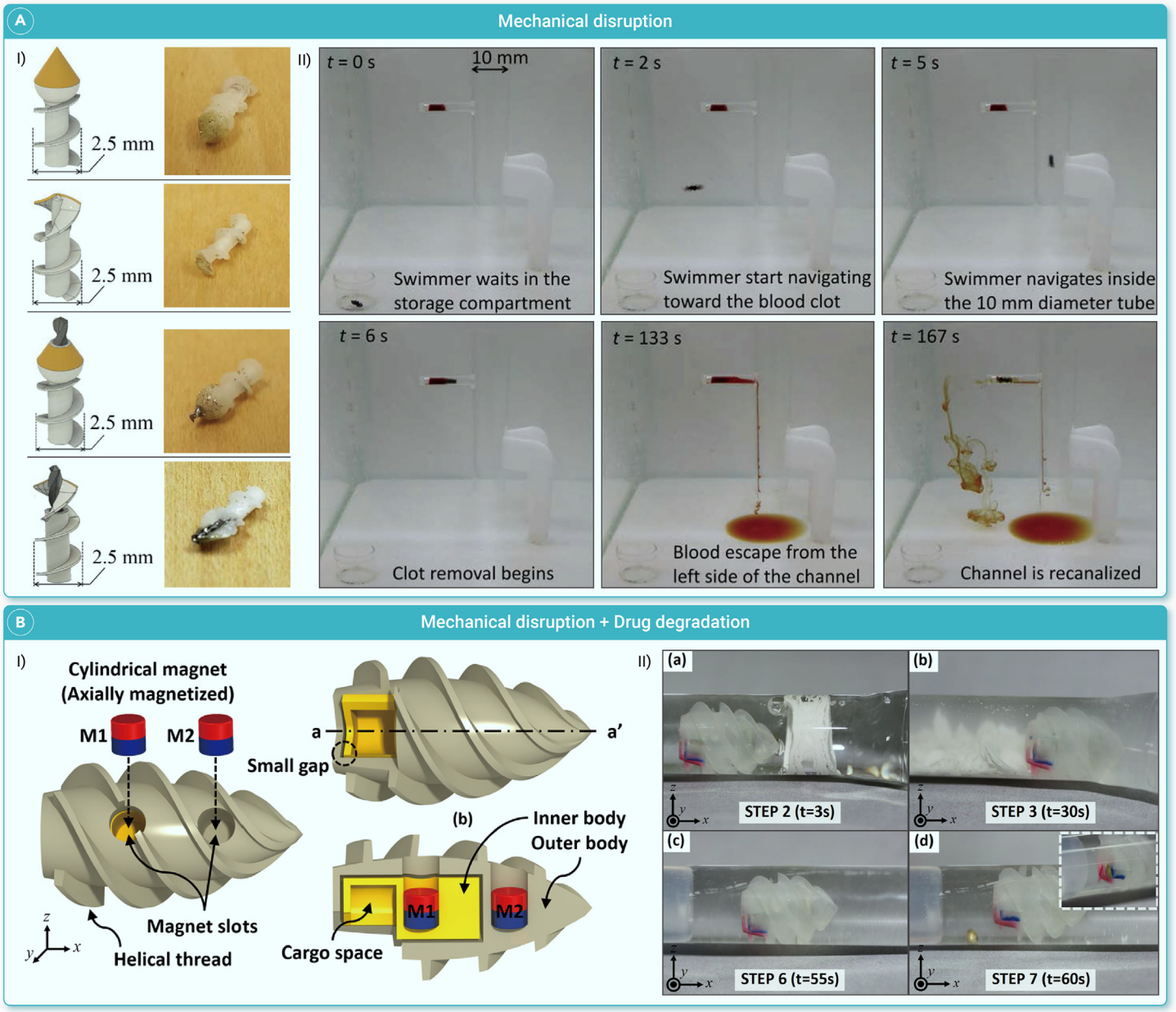

Figure 5. Thrombus removal using millimeter-scale robots Two typical examples of millimeter-scale robots for thrombus removal by mechanical disruption (A)[148] (Copyright 2020, IEEE) and a combination of mechanical disruption and chemical degradation (B).[163] Copyright 2015, AIP.

thermal ablation (Figure 6B).[75] However, overcoming the limited penetration of light in biological tissues remains challenging. In comparison, sonodynamic therapy that utilized ultrasonication of O_2 bubbles enabled the cavitation effect for generating mechanical force, which effectively enhanced the deep penetration of thrombolytic agents into thrombi (Figure 6C). Similar to millimeter-scale robots, microrods can damage blood clots via direct mechanical interaction controlled by an external magnetic field (Figure 6D), although their thrombus removal efficiency was constrained by its relatively weak force output. Chemical lysis of blood clots was commonly achieved by designing robots for drug loading and release. For instance, a platelet membrane (PM) medicated nanorobot was designed for sequential drug release of the thrombolytic urokinase and anticoagulant heparin (Figure 6E).[57] Such nanorobots could target the thrombus site enabled by special proteins on the PM, which was then ruptured by NIR irradiation for sequential drug release. While localized drug accumulation can be achieved using micro/nano-scale robots, the thrombolysis effect is limited when it relies solely on chemical lysis. To overcome this limitation, Wang et al. developed swarming tPA-nanorobots that effectively clear blood clots by combining mechanical interaction, chemical lysis, and hydrodynamic convection (Figure 6F). tPA-nanorobots were rapidly delivered to the site near the narrow branch (submillimeter-scale segments) occluded by the blood clot. The swarming tPA-nanorobots were then released from the catheter and magnetically navigated to the thrombus for targeted thrombolysis. The intervention procedure was guided in real time using clinical fluoroscopy imaging, ensuring precise and safe deployment of the tPA-nanorobots. After successful recanalization, tPA-nanorobots returned to the catheter for retrieval, which may minimize potential side effects (e.g., secondary occlusion and long-term toxicity). This approach presents a promising strategy for tackling thrombi in the M3/M4 segments using a nanorobotic-based therapeutic platform that integrates the actuation system with the clinical imaging modality, potentially strengthening treatment outcomes of patients with AIS.

Based on the advancement of previous studies, here we summarize the three modes of drug delivery, as well as the main mechanism of thrombus removal by using MRs, to highlight potential approaches for improving treatment efficiency. MRs can deliver drugs to the clotting region in three modes (Figure 7A). In mode 1, the drug is coated into the MRs via chemical binding, enabling them to directly perform the thrombolysis once they arrive at the thrombus. Precise and robust control over MRs is vital for ensuring the MRs remain anchored to the thrombus, which allows sustained thrombolysis. This highly localized process can not only

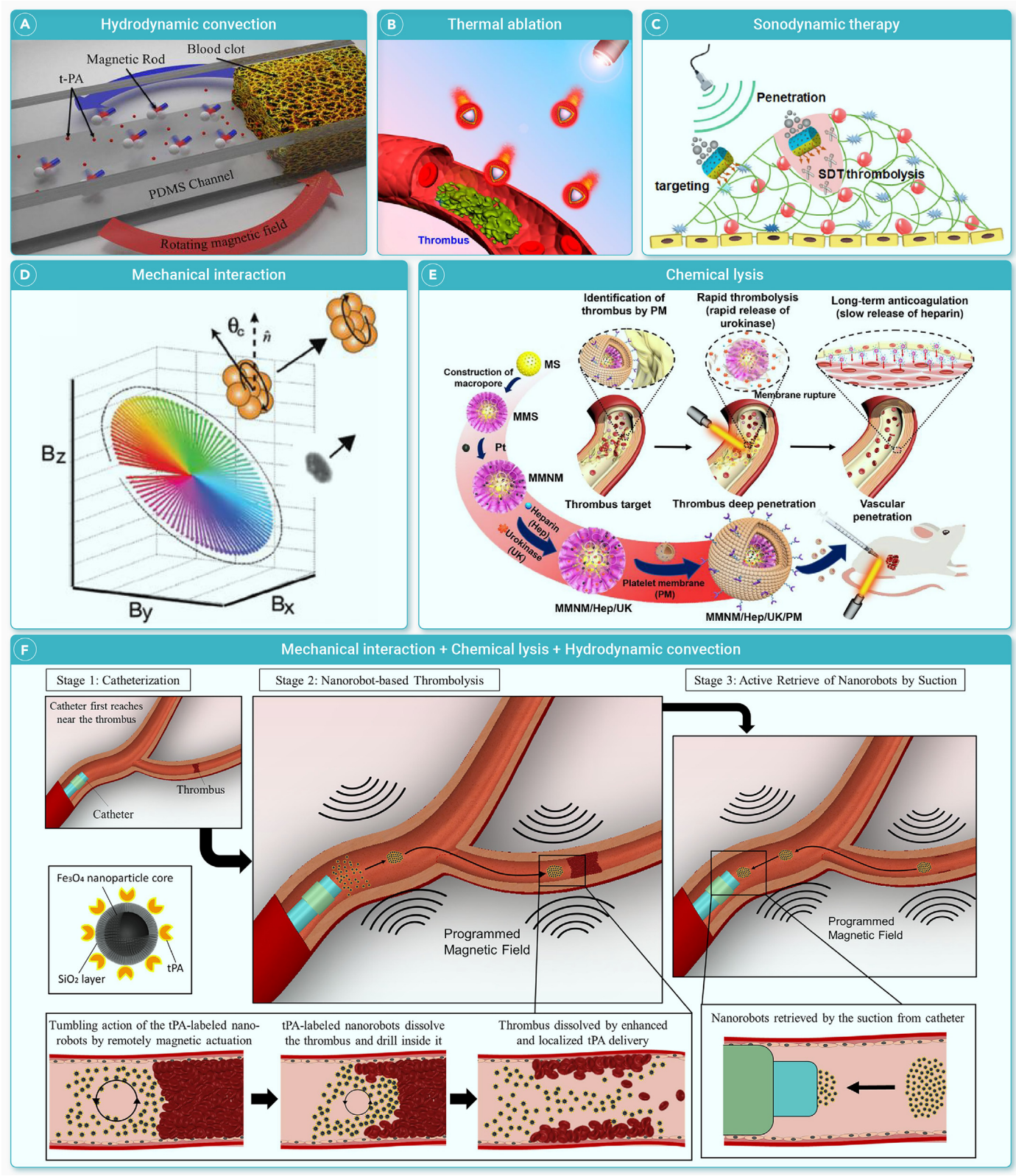

Figure 6. Mechanisms of thrombus removal using micro/nanometer-scale robots Various thrombus removal mechanisms, including (A) hydrodynamic convection,[149] Copyright 2014, American Chemical Society; (B) photothermal ablation,[75] Copyright 2018, American Chemical Society; (C) sonodynamic therapy,[153] Copyright 2021, American Chemical Society; (D) mechanical interaction,[151] Copyright 2017, WILEY-VCH; (E) chemical lysis,[57] Copyright 2020, The Authors; and (F) mechanical interaction with chemical lysis and hydrodynamic convection.[3] Copyright 2024, The Authors.

minimize drug dosage but also maximize treatment efficiency. In mode 2, MRs serve as carriers for therapeutic agents, transporting drugs to the targeted clotting region. Drug release can then be triggered by stimuli, such as NIR radiation,[57] magnetic hyperthermia,[133] and reactive oxygen species (ROS).[166] However, a great limitation of this strategy is the potential that the released drugs may diffuse away from the clot, diminishing thrombolysis efficiency. Moreover, the short therapeutic window of AIS requires quick drug release and access to the clotting region. Mode 3 involves the systemic distribution of the drug through the bloodstream, with MRs subsequently pumping the drug toward the clot under external actuation (e.g., rotating magnetic fields). Although this approach

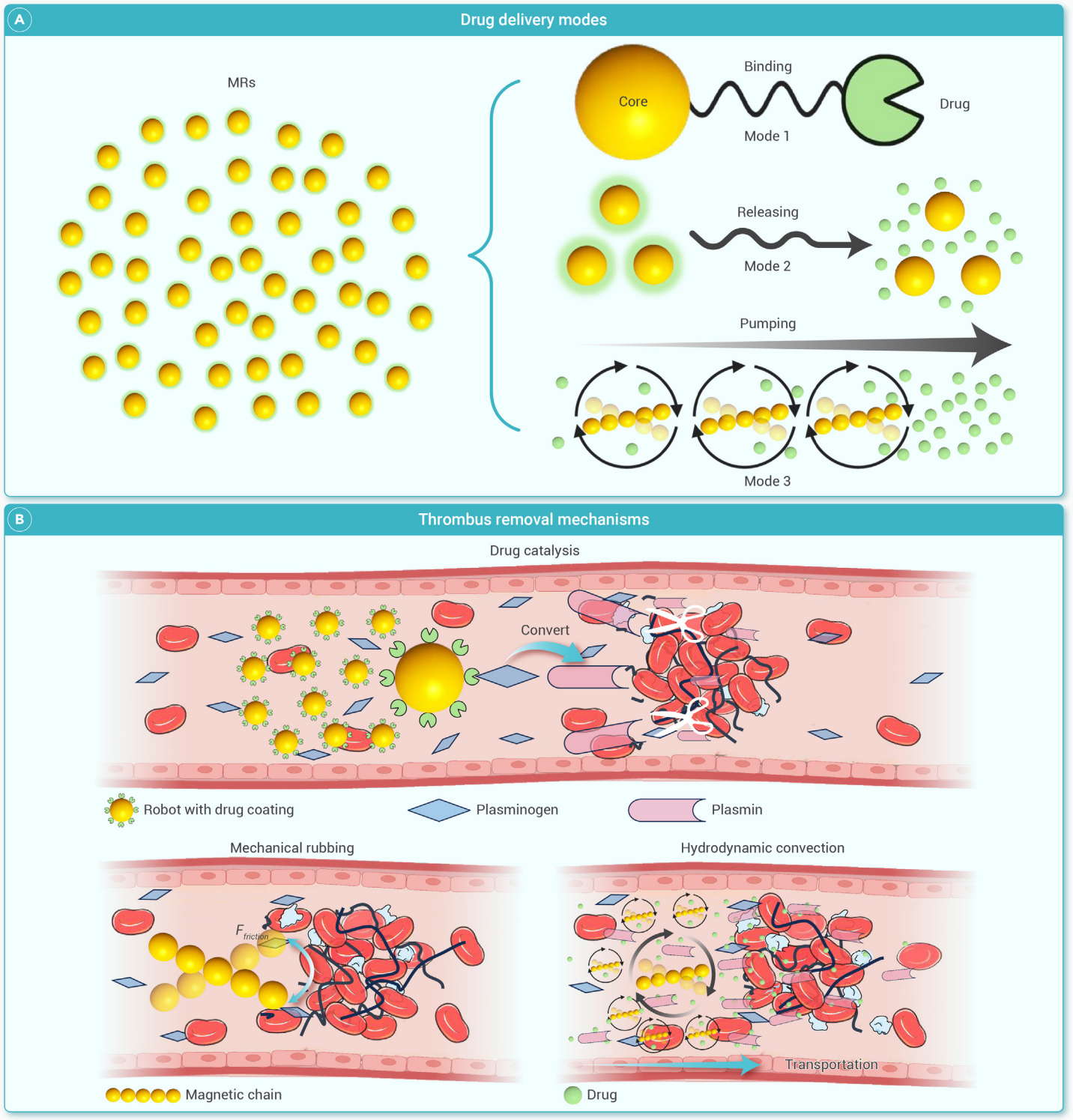

Figure 7. Drug-delivery modes and blood-clot removal mechanisms (A) The scheme of thrombus removal using MRs with three drug-delivery modes. (B) Scheme of primary thrombus removal mechanisms, including enzyme catalysis, mechanical rubbing, and hydrodynamic convection.

allows for large-ranged drug distribution, high drug dosages are required to maintain sufficient concentration levels, which increases the risk of acute side effects (e.g., SIH). Among these modes, the first offers great potential for achieving rapid recanalization while minimizing the drug dosage and reducing associated side effects. Besides precise drug delivery, an in-depth understanding of the mechanisms of thrombus removal is necessary to further improve therapeutic outcomes. Enzyme catalysis (chemical lysis) plays a key role in thrombus degradation by converting PLG into PLM and enabling fibrinolysis. This process can be activated by thrombolytic drugs (typically, tPA or urokinase) loaded onto MRs. Two methods can potentially be adopted to boost the enzymic degradation of thrombus. First, improving the local concentration of thrombolytic drugs could accelerate plasmin conversion benefiting the fibrin degradation, which can be achieved by precise actuation of MRs to the thrombus.[150] Second, incorporating thrombolytic drugs with higher activity into MRs can also enhance the degradation efficiency. For example, the third-generation thrombolytic drug reteplase has demonstrated a better recanalization effect in clinical practice[167]; thus, the thrombolysis effect of MRs combined with newly developed drugs is worth investigating in the future. In addition to chemical degradation, MRs can disrupt thrombi mechanically by generating frictional forces, as shown in the lower left part of Figure 7B. This mechanism is commonly applied for magnetic-driven

MRs, where rotation or corkscrew-like motion generates friction force upon direct contact with the clot, contributing to mechanical damage.[63,151] As thrombi become denser and stiffer over time, the mechanical rubbing effect of MRs may be constrained during long-term interaction. Consequently, combining mechanical disruption with enzymatic lysis can produce a synergistic effect, dramatically improving thrombus removal efficiency. Previous studies have confirmed that the thrombolysis rate of robots with a synergetic effect improved more than 100 times compared to those utilizing only mechanical rubbing or enzyme catalysis.[3] Beyond the aforementioned mechanisms, the motion-triggered hydrodynamic convection of MRs (the lower right part of Figure 7B) could enhance drug diffusion into deeper regions of the clot and promote thrombus degradation. For example, Zhao et al. reported that a 2-fold improvement in thrombolysis rate was realized by the hydrodynamic convection using swarming nanorods under an external magnetic field.[149] Similarly, ultrasound-induced bubble cavitation has also been investigated to prompt drug diffusion and thrombus disruption, although adverse effects associated with bubble generation should be prevented. Altogether, the thrombolytic performance of MRs can be further enhanced by combining enzyme catalysis, mechanical disruption, and hydrodynamic convection along with precise actuation and motion control.

Moreover, the thrombus microenvironment presents several significant challenges, including elevated levels of ROS, acidic pH, high shear stress, increased thrombin concentration, and the structure and composition of a clot. Each of these factors profoundly impacts the design and performance of MRs, as outlined below.

(1) ROS concentration: elevated levels of ROS in thrombotic regions contribute to oxidative stress, which can damage surrounding biological tissues and cells, exacerbating neurological deficits.[168] ROS can disrupt the neurovascular unit, increase blood-brain barrier (BBB) permeability, and even lead to hemorrhagic transformation.[169] Excess ROS can serve as an internal stimulus for triggering drug release. For instance, Quan et al. demonstrated a system that combined cold-shock platelets with ROS-responsive liposomes via host-guest interactions, which selectively accumulated at thrombus sites and released therapeutic drugs rapidly in response to high ROS levels.[170] In addition to thrombolysis, MRs can also be employed to clear excess ROS. Cheng et al. synthesized a multifunctional amphiphile combining low-molecular-weight heparin, tempol, and linoleic acid (LA), which self-assembled into nanoparticles. These nanoparticles can simultaneously dissolve thrombi and scavenge ROS, addressing inflammation and oxidative stress.[171]

(2) pH variations: in ischemic strokes caused by cerebral thrombosis, acidosis can lower the pH in the ischemic region.[172] The acidic pH typically observed in thrombotic regions can negatively affect the activity of thrombolytic agents delivered by MRs, such as tPA, whose efficacy diminishes in low-pH environments. To address this challenge, pH-responsive systems have been developed using materials that activate or stabilize thrombolytic agents under acidic conditions. For instance, Nagasaki et al. encapsulated tPA in polyion complex nanoparticles composed of polycation and polyanion. These nanoparticles rapidly collapsed under acidic conditions, effectively releasing tPA to dissolve thrombi.[173]

(3) High shear stress: one of the most significant physical changes in the pathological microenvironment of a thrombus is the sharp increase in blood shear force at the thrombus site. Normal arterial blood flow shear stress ranges from 10 to 70 dyne/cm^2, whereas, in stenotic regions caused by thrombi, shear stress can exceed 1,000 dyne/cm.[174] For example, when coronary artery obstruction exceeds 75%, the local shear stress at the thrombus site increases by up to 53 times.[174] On the one hand, such high shear stress can hinder the MR's ability to navigate and anchor effectively at the clot site. Magnetic-field-actuated MRs have demonstrated the ability to counteract these forces, enabling precise targeting and retention even under challenging conditions; on the other hand, high shear stress has also been leveraged to achieve localized release of thrombolytic drugs at the thrombus site, enhancing thrombolysis efficacy and reducing the risk of systemic bleeding. Netanel et al. firstly proposed that utilizing high shear stress at thrombus sites for specific drug delivery. They developed shear-sensitive tPA-nanoparticle aggregates that disintegrated within 10 min under high-shear conditions, effectively restoring hemodynamics in a mesenteric injury model and improving survival rate in a fatal mouse pulmonary embolism model. Similarly, Zhang et al. constructed shear-responsive core-shell nanoparticles through β-cyclodextrin host-guest interactions. The sharply increased shear stress at the thrombus site disrupted the core-shell structure, triggering the rapid release of urokinase and achieving site-specific thrombolysis.[175]

(4) Thrombin concentration: elevated thrombin levels within the thrombus contribute significantly to its structural stability and resistance to lysis. MRs designed to locally deliver thrombin inhibitors or modulate thrombin activity can destabilize the clot, making it more susceptible to thrombolysis. In addition, thrombin, as a key coagulation signal in the pathological progression of thrombosis, can be utilized to design "closed-loop" controlled release strategies. For example, Xu et al. developed a thrombin-cleavable peptide as a crosslinker to create a self-regulating nano-scale polymeric hydrogel loaded with hirudin. This system adaptively released encapsulated hirudin in response to thrombin concentration changes during thrombosis, enhancing anticoagulant activity while reducing adverse effects.[176]

(5) The structure and composition of clot: the heterogeneous composition of thrombi, including fibrin networks and blood cells, can significantly impede MR penetration and movement. Newly formed thrombi typically have a loose fibrin network, making them easier to dissolve. However, as thrombi become "older," their structure hardens, the fibrin network becomes denser, and platelet contraction within the cross-linked clot causes thrombus retraction and stabilization. Additionally, disk-shaped red blood cells compress into polyhedral cells, further increasing thrombus density and resistance to thrombolysis. This makes it more challenging for MRs to penetrate and exert their thrombolytic effect. This issue can potentially be addressed by combining thrombolysis with physical interactions (e.g., mechanical rubbing and sonodynamic cavitation).

As previously discussed, researchers have developed various methods to enhance MR penetration into thrombi, including magnetic, US, and light-based strategies. Furthermore, specific proteins within the thrombus structure can serve as targets to improve MR penetration. For example, peptides that bind to fibrin or activated platelets can effectively enhance MR adhesion and therapeutic efficacy, and common examples include CREKA,[177] cRGD,[153] and platelet membranes.[178]

CLINICAL TRIALS

Creighton's group conducted clinical trials using magnetic nanoparticles (MNs) to improve tPA diffusion for treating acute stroke in patients.[179] Seven patients suffering from AIS were enrolled in a safety and feasibility study targeting large-vessel intracranial occlusions. These AIS patients aged 63 to 91 years were treated with an i.v. injection of tPA combined with MNs within 4.5 h of symptom onset. A magnetically enhanced diffusion (MED) device was developed that enables the assembly of magnetic chains, acting as micropumps to transport tPA to the occlusive branch, thereby accelerating recanalization. Angiography indicated that complete recanalization was realized in all patients. These clinical results, demonstrating complete recanalization in seven patients with AIS, highlight the translational potential of MRs. However, larger-scale trials are needed to validate their efficacy and long-term safety.

Integrating MRs into existing surgical procedures is essential for transitioning them from the lab to the operating room. This approach can minimize operational difficulties for clinicians and facilitate rapid recanalization for patients. The development of MRs should align with real clinical needs and aim to simplify procedures for clinicians who perform surgical interventions. However, the workflow of intervention procedures combining MRs with designed actuation systems in a real clinical scenario remains unclear. Here, we use AIS as a typical example to propose a potential workflow for integrating MRs and actuation systems to achieve precise and effective treatment, as depicted in Figure 8. When a patient potentially suffering from AIS arrives at the hospital, diagnostic imaging is performed to identify and localize the thrombus within the cerebral vasculature by imaging test (e.g., fluoroscopic angiography). Digital subtraction angiography

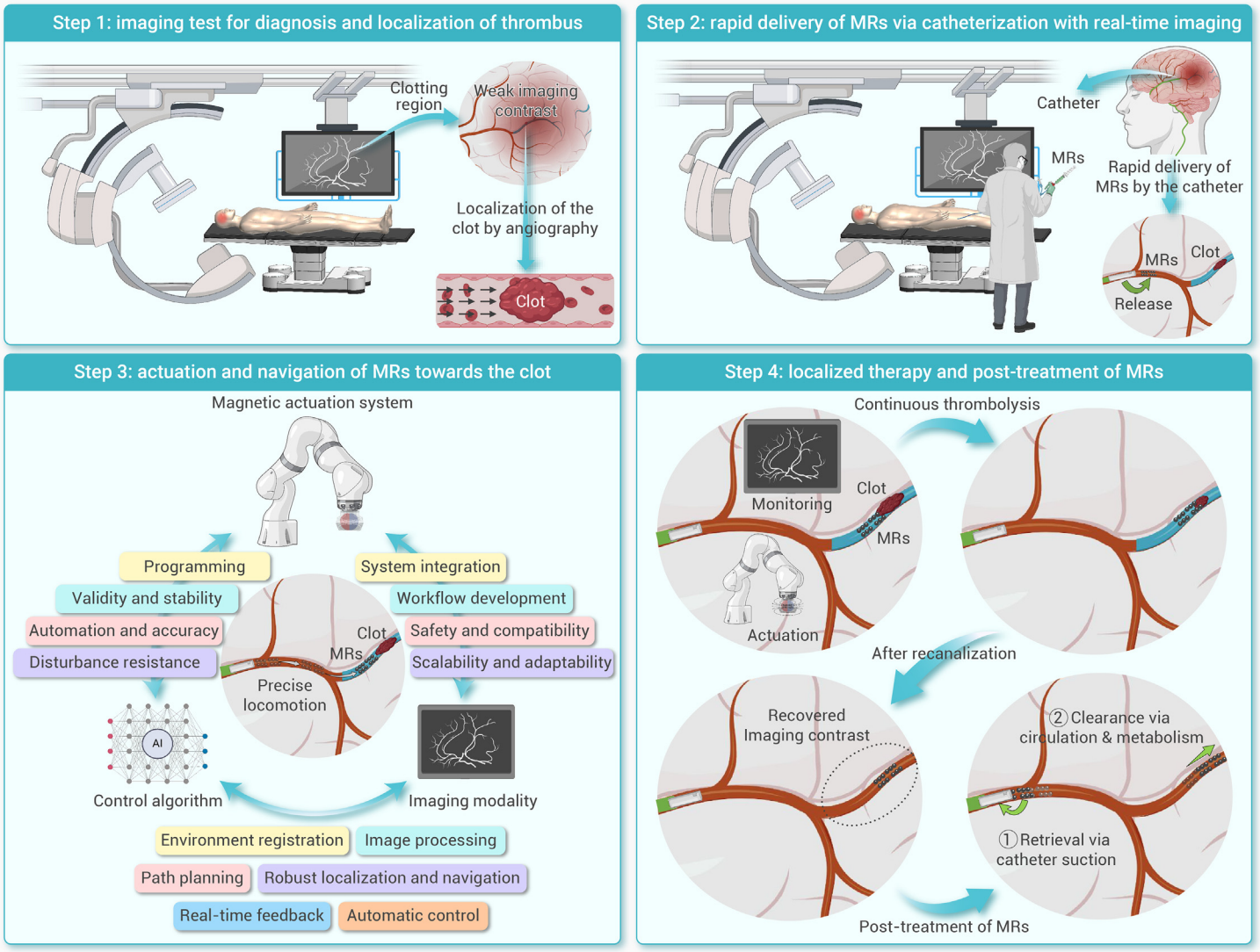

Figure 8. Schematic of detailed intervention procedures using MRs for ischemic stroke treatment Part of the schematic was created using BioRender.com.

(DSA) can generate 3D anatomical images of the cerebral vasculature, facilitating smooth catheterization and precise actuation of MRs in subsequent procedures.[178] In step 2, catheterization is conducted by clinicians to rapidly deliver MRs over a long distance, typically from the patient's limb to the brain under fluoroscopy imaging guidance. After reaching the vicinity of the branched vessel occluded by the thrombus, MRs are released from the catheter via injection. To mitigate blood flow disturbance, a catheter balloon can be inflated to temporarily reduce or halt blood flow, ensuring highly reliable deployment of MRs. Simultaneously, remote and precise actuation can be conducted, allowing controllable locomotion of MRs toward the clot. As discussed elsewhere in this article (actuation of MRs), magnetic actuation systems represent one of the most suitable options for navigating MRs in narrow and complex environments. In this regard, the actuation system plays a crucial role in determining the physical targeting ability of MRs and the treatment outcome, necessitating proper integration with compatible imaging tools. The design of the actuation system must ensure that its deployment does not interfere with the normal functioning of imaging modalities. Some key parameters, such as working space, distance, size, and spatial position, require comprehensive technical consideration. Safety is also a major concern, and the developed actuation system should pose no risks to either the patient or the clinician. Electromagnetic systems generally possess higher safety than permanent magnet-based systems, owing to their programmable properties, instant "on-off" switch, and relatively low force output. For example, Nelson et al. developed an electromagnetic system for dexterous navigation of a catheter robot with improved endovascular access in live pigs, showing great potential for AIS treatment in clinical settings.[180] When MRs decrease to the micro/nano scale, reliable actuation becomes significantly challenging, as a large magnetic field strength is required to overcome the drag force of blood flow. Although balloon catheters can reduce or halt blood flow temporally, long-term intervention is not feasible. Therefore, employing permanent magnet-based systems may be inevitable to provide sufficient magnetic field strengths for effective navigation of micro/nanorobots.[181] Balancing safety concerns with the need for strong magnetic fields depends on the specific type of MRs and their intended applications. Moreover, accurate algorithms are another key component of the actuation system, enabling automatic control of MRs without or with minimal manual manipulation.[182,183] Sophisticated manual operation may impose a heavy training burden on clinicians, compromising the popularity of these systems for clinical deployment. MR-based therapeutic platforms are designed to simplify surgical procedures and improve treatment outcomes, rather than replace clinicians, as failure to consider this issue could lead to clinical rejection.[58] The algorithm should dynamically adjust the magnetic field generation and actuation modules to facilitate accurate locomotion of MRs within endovascular lumens. Algorithm-guided navigation of MRs greatly relies on real-time imaging feedback. Images of complex 3D vascular structures obtained from imaging modalities can be transferred to an algorithm module for image processing, environment registration, and path planning procedures, which facilitates robust localization and navigation of MRs.[184,185] With the rapid development of artificial intelligence (AI), such a capability is becoming progressively attainable. For example, Choi et al. adopted reinforcement learning with a gradual training approach to achieve autonomous 3D positional control of a magnetic microrobot in an ever-changing vascular environment, showing a sense of

generality and adaptability.[183] Taken together, precise and effective actuation and navigation of MRs in dynamic and complex 3D endovascular environments require tight coordination between reliable actuation systems, imaging modalities, and robust algorithms.

After arriving at the thrombus site, MRs will perform continuous thrombolysis with magnetic actuation and imaging monitoring, as shown in step 4. Strategies to improve efficiency have been discussed elsewhere in this article based on the thrombus-removal mechanisms. Besides, the parameters of the magnetic field can also impact treatment efficiency. For example, the thrombolysis rate of tPA-nanorobot swarms varies with the frequency of the external magnetic field. Improper input frequency setting may result in insufficient force output or an overly vigorous swarming state, which attenuates both the mechanical interaction and the hydrodynamic convection, consequently reducing the thrombolysis rate.[3] Similarly, the magnetic field strength can also mediate the thrombolysis process by influencing the motion behavior of MRs. Therefore, a well-developed actuation system should ensure the precise and reliable navigation of MRs while simultaneously enhancing thrombolysis efficiency through optimized parameter management. Following successful recanalization, post-treatment of MRs emerges as a critical concern. Two potential approaches are proposed as depicted in the lower right part of Figure 8. MRs can be cleared from the body through circulation and metabolism, necessitating a comprehensive assessment of the physicochemical properties of MRs. Meanwhile, technical standards, such as operational procedures, applied external fields, retrieval mechanisms (e.g., magnetic attraction or catheter suction), and monitoring and feedback strategies, should be established to enable the safe and active retrieval of MRs.

Although this review mainly focuses on using MRs for ischemic stroke treatment, it should be emphasized that therapy strategies may vary depending on the location of the clot. For example, MRs are not suitable for treating thrombus-induced myocardial infarction due to the high blood flow, which can lead to instability and uncontrollability of the MRs. In contrast, tethered robots may offer viable solutions for thrombus removal in such larger endovascular lumens.[186–188] For thrombi formed in soft tissues such as those associated with deep vein thrombosis and atherothrombosis, portable US imaging can be employed for visualization and monitoring, eliminating the radiation risks of X-ray-based imaging modalities. This approach could also benefit patients without access to hospitals equipped with costly imaging technologies (e.g., fluoroscopy). In some cases, clots in the deep veins of the leg or pelvis may fragment into multiple pieces, potentially traveling to the lungs and causing pulmonary embolism across various vessel branches. Therefore, simultaneous control of multiple MRs to remove the clots in various pulmonary vessels is crucial for fast recanalization, requiring specialized design for both the actuation systems and the MRs. Taken together, thrombosis could occur in various organs and tissues, and, to achieve optimal therapeutic outcomes, the intervention strategy involving MRs, actuation systems, and imaging methods must be customized to adapt to various clinical scenarios.

It is also important to conduct a comparative analysis of MRs versus traditional methods in terms of accessibility, efficacy, and cost, highlighting the necessity for clinical translation of MRs. MRs can navigate through the vascular system with high precision, physically and specifically targeting thrombosis regions. This unique capability offers MRs exceptional accessibility, especially in small and tortuous vascular lumens, where thrombectomy devices often struggle to reach. Moreover, the small size of MRs minimizes trauma to fragile blood vessels, further reducing damage to surrounding tissues. Ensuring the safety of the intervention procedure is challenging for thrombectomy-based therapy when treating ischemic stroke in the human brain. Clinical reports indicate that the risk of all-cause mortality associated with thrombectomy, including brain damage, is approximately 17%.[189] MRs are potentially able to lower the mortality rate associated with undesired surgical complications of thrombectomy, due to their safety and dexterous accessibility. Compared with clinical drug-based thrombolysis, the mobility of MRs offers an obvious benefit of localized therapeutic capability, which can minimize drug dosage and lower the risk of SIH. Importantly, MRs can promote clot degradation through a combination of mechanical interaction and chemical lysis, demonstrating superiority over traditional thrombolysis in terms of higher efficiency and reduced drug administration. Based on the report from a clinical trial, nearly one-third of patients failed to achieve recanalization within 2 h using standard tPA-based thrombolysis.[70] In comparison, many MR-based therapeutic platforms have shown the potential to significantly prompt the recanalization efficiency.[3,150,152,157] However, most laboratory research has been primarily conducted on animals, with limited attempts involving clinical treatments.[179] More preclinical and clinical studies are required to validate the thrombolytic effect and the treatment outcome of MRs in clinical settings. Another important factor is the cost, which determines the commercialization potential of MRs. The initial investment required for MR-based platforms, including design, optimization, and upgrading, is relatively high. MR-based therapeutic platforms demonstrate considerable potential for long-term cost savings by reducing hospital stays and complications, thereby alleviating financial burdens on patients. Moreover, unlike traditional methods, MR-based platforms enable remote and teleoperated procedures, which may significantly improve their accessibility in underserved areas.[181,190] For example, Zhao et al. demonstrated real-time teleoperation using a Joystick controller with fluoroscopy imaging, showing effective and time-saving performance. In summary, MRs present a promising alternative to traditional thrombus treatment methods, offering advantages in precision, efficiency, and remote operation.

Furthermore, a potential pathway for the clinical translation of MRs designed for endovascular recanalization is proposed (Figure 9) to provide an actionable framework for researchers and related practitioners. The pathway begins with basic research to establish fundamental groundwork. This phase involves developing and optimizing the design of MRs, including structure, imaging contrast, functionality, biocompatibility, and other relevant factors. In this stage, an initial prototype of the actuation system should be developed to assess the controllability and thrombolysis performance of the MRs. Next, the focus shifts to the proof-of-concept verification phase, during which the integrated system is evaluated through *in vitro*, *ex vivo*, and small-animal models. This phase aims to validate the feasibility and functionality of MRs in laboratory settings. The progression then advances to the preclinical studies phase, where the performance and workflow of MR-based thrombus treatment are rigorously tested in large-animal models (e.g., pigs). This stage is crucial for optimizing the integrated system and ensuring the safety and reliability of MR-based technology in human-like environments. The clinical trial phase is a pivotal milestone. In this phase, the MR-based platforms will undergo comprehensive testing and evaluation in human trials, solidifying their clinical viability. The ultimate goal is to achieve population-level outcomes, where MR-based technology is transferred to industrial manufacturing and adopted in hospitals, delivering tangible benefits to patients and society. Throughout this multifaceted pathway, the development of MR-based therapeutic platforms for endovascular recanalization is guided by a systematic and evidence-based approach, ensuring their safety, efficacy, and feasibility for clinical translation.

CONCLUSION AND OUTLOOK

The concept of MRs that can navigate inside the human body to treat vascular blockages has been envisioned for almost half a century, initially popularized in the science fiction film *Fantastic Voyage* (1966). Significant advancements have been made by the research community to bring this vision closer to reality. Various types of MR have demonstrated their viability in thrombus removal, ranging from laboratory studies to clinical trials. In this section, we summarize the challenges and future directions for using MRs in thrombus treatment, including performance optimization, delivery strategies, tracking and imaging approaches, and safety issues, to clarify the translational perspective of MRs.

Challenge 1 involves precise navigation of MRs in complex and dynamic 3D vascular environments, which remains one of the fundamental challenges for achieving effective recanalization outcomes, especially in cerebral regions. Major obstacles include the strong disturbances induced by high blood flow, material selection, real-time imaging feedback, robust actuation strategies, and reliable algorithm support. Regarding future orientation, magnetic-driven MRs represent one of the most promising options for thrombus treatment, owing to their remote controllability, safety, programmability, deep tissue penetration, and so on. To overcome the disturbances induced by high blood flow, it is essential to apply sufficient magnetic field gradients that enable MRs to effectively resist drag forces. This can potentially be achieved through well-designed permanent magnet-based systems with larger dimensions or electromagnetic systems with enhanced magnetic induction intensity by integrating the iron core. Moreover, the development of novel actuation strategies may offer enhanced navigation precision. For instance, Li et al. demonstrated human-scale navigation of magnetic microrobots in hepatic arteries by utilizing the alignment between the gravity of microrobots

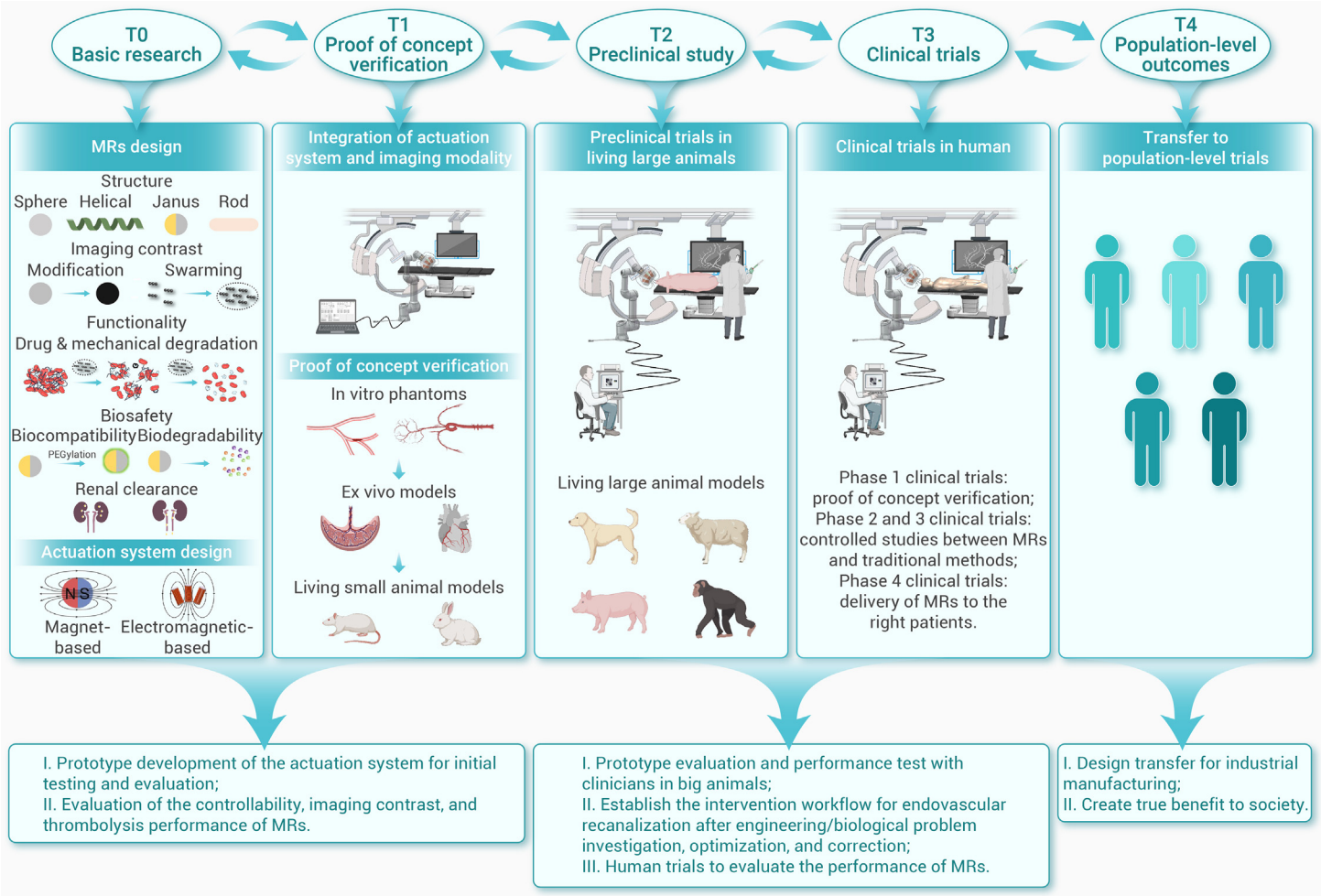

Figure 9. A proposed pathway toward clinical translation of MRs designed for endovascular recanalization Part of the schematic was created using BioRender.com.

and the orientation of the magnetic field.[191] Additionally, employing existing intervention techniques to temporarily reduce blood flow, such as catheter balloon expansion, presents a feasible and effective approach to support MRs deployment. Constructing MRs from materials with high magnetic saturation, such as Fe_3O_4, FePt, or carbonyl iron, is another straightforward method to ensure excellent magnetic responsiveness and resistance to high drag forces. Meanwhile, imaging plays a critical role in guiding MRs to precisely accumulate at the blood clot site with real-time feedback. The integration of actuation systems with clinical imaging modalities is therefore necessary. Currently, fluoroscopy imaging is one of the optimal candidates for integrating with the magnetic actuation system due to its high temporal and spatial resolution, flexible positioning capabilities, sufficient working space, and adaptability in clinical environments. The design of magnetic actuation systems should align with the deployment of fluoroscopy imaging to ensure compatibility. At the same time, portable imaging tools such as US imaging could serve as supplementary guidance systems, offering the advantage of avoiding radiation risks. Last but not least, the advancement of AI-based algorithms, such as machine-learning and deep-learning methods, has demonstrated the ability to enhance the autonomous recognition and precise navigation of MRs within endovascular environments.[184,185] For example, machine learning can analyze vast datasets derived from medical imaging and real-time inputs to develop predictive models that anticipate changes in vascular landscapes, benefiting flexible MR navigation. Combining intelligent algorithms with advanced robotic systems is a pioneering step toward the future of using MRs for minimally invasive endovascular interventions.

Challenge 2 is that treatment outcomes are significantly determined by the thrombolysis performance of MRs, raising another challenge in improving thrombus removal efficiency. Although many mechanisms have been explored to accelerate thrombus removal, there is still a lack of solid verification from preclinical or clinical trials, resulting in a huge gap between laboratory studies and real-world adoptions. Regarding future orientation, strategies can be considered to further boost the thrombolysis effect of MRs. (1) On the one hand, locally improving the concentration of thrombolytic drugs would accelerate the enzyme conversion for fibrinolysis; on the other hand, developing novel thrombolytic drugs with higher activity and incorporating them into MRs may promote the degradation efficiency. (2) Strengthening the mechanical interaction between MRs and thrombi contributes to a faster breakdown of the fibrin matrix. This can be achieved through proper structure design of MRs (e.g., adopting helical structures or creating coarse surfaces to improve force output or interface interactions) or by inducing local swarming motion behavior of collective MRs.[154] Moreover, the parameter setting of the magnetic actuation system, e.g., magnetic field frequency, strength, and orientation, plays a critical role in motion behavior regulation, necessitating further investigation and optimization. (3) Enhancing drug diffusion within the thrombus is another approach to facilitate a faster thrombolysis process. Possible strategies include triggering hydrodynamic convection through MR motion control or imposing external stimuli such as acoustic radiation. (4) To bridge the gap between laboratory research and clinical deployment, future studies should prioritize comprehensive preclinical evaluation of MR-based platforms in large-animal models, including safety profiling, therapeutic efficacy, and pharmacokinetic analysis. Subsequently, these findings must undergo validation in human trials through established clinical translation pathways rather than relying on preliminary *in vitro* demonstrations.

Challenge 3 is that the blood circulation system spans a long distance over the meter scale, whereas most previous studies have only demonstrated short-distance delivery. In this regard, proper long-distance delivery strategies for MRs must be taken into consideration. For example, direct injection-enabled circulation of MRs is an inefficient delivery method, considering the undesired loss or accumulation in the non-targeted blood vessel branches, making it unsuitable for effective MR delivery. Although MR techniques can perform high-precision

navigation toward the thrombus region, the locomotion of MRs, particularly for micro/nano-scale robots, over the human-body range is time consuming, which may exacerbate the patient's condition due to delayed treatment. Regarding future orientation, to overcome the time delay caused by long travel distances, catheterization can be utilized to rapidly deliver MRs, which requires rational design of both MRs and the catheter. For example, specialized coatings can be applied to the catheter walls to reduce friction, facilitating the smooth transportation of MRs and preventing potential adhesion.[192–194] The physical and chemical properties of MRs should be compatible with the catheterization process. The physical properties of MRs mainly include size, shape, surface electronegativity, and mechanical strength. The dimensions of MRs must match the inner diameter of the catheter; smaller MRs can move flexibly within the catheter, reducing the risk of stacking or complete occlusion during transportation. The shape of MRs can be optimized to enhance their stability within the catheter; e.g., a streamlined design of MRs can minimize fluid resistance, improving transport efficiency.[195] Surface electronegativity of MRs also affects their interactions with the catheter wall and other components in the bloodstream.[196–198] By adjusting electronegativity, static attraction can be minimized, reducing adhesion to the catheter and facilitating the transport process. Mechanical strength and flexibility of MRs are also important factors; using high-strength yet soft materials allows MRs to adapt to the twisted and narrow lumen of the catheter.[199,200] For the chemical properties of MRs, surface modification plays a key role in improving delivery efficiency. For example, increasing hydrophobicity via chemical modifications may reduce interactions with catheter components and lower adhesion risks.[53] Additionally, the chemical stability of MRs in liquid environments (e.g., saline or blood) is essential to prevent undesired reactions that may compromise delivery efficacy.[201]

Challenge 4 is that the disposal and safety of MRs are critical issues after treatment, as long-term circulation of those therapeutic agents inside vessels may cause secondary blockages and other side effects. Ensuring the biocompatibility of MRs alone is insufficient to meet the rigorous standards for clinical use in vascular environments, especially in the cerebral regions. Regarding future orientation, to remove MRs from vessels after recanalization, the following strategies could be adopted: (1) Scaling MRs down to a size smaller than 100 nm allows rapid clearance of MRs by renal pathways. (2) Applying biodegradable materials to fabricate MRs enables their gradual degradation after treatment, thus reducing the risk of long-term retention in the body. Achieving this goal requires thorough investigations into how the designed materials interact with the blood environment, including their degradation kinetics, mechanisms, and biosafety of degradation byproducts. (3) Beyond passive removal methods, active retrieval of MRs post treatment warrants exploration. Catheter-based techniques can directly extract MRs from vasculature via suction, while magnetic stent-assisted strategies may enable targeted capture at specific sites. These approaches are critical for MRs with limited size-reduction capacity; for example, magnetic-driven MRs experience diminished controllability and propulsion when scaled down due to reduced magnetic volume. Ultimately, safe and effective post-treatment depends on MRs' size thresholds, material properties, and actuation types, necessitating comprehensive analysis and evaluation.

Challenge 5 is that most previously reported MRs are actuated individually, meaning that they operate in a dispersed state inside the vessel. Such a control strategy often leads to a substantial number of MRs entering downstream vessels without encountering blood clots, potentially compromising their targeting ability. Regarding future orientation, compared to the delivery of individual agents, swarming motion and control of active matter are promising for transporting large doses of drugs, cargo materials, cells, and energy conversion with a single delivery.[202,203] By enhancing the targeting capabilities of swarming MRs within complex 3D branched vascular systems, it is possible to significantly decrease the demanding dosages of therapeutic agents, thereby minimizing the associated side effects.[204,205] Moreover, the swarming motion of MRs is often accompanied by stronger mechanical interaction with targeted objects, leading to enhanced drug diffusion and large force output. Lastly, inducing the swarming behavior of MRs is an effective method to significantly enhance or enable imaging contrast in physiological vasculatures, guaranteeing precise navigation and targeting. Taken together, the swarming behavior of MRs can not only reduce the drug dose but also facilitate recanalization, which needs future in-depth exploration in terms of swarming mechanisms, precise regulations, and multi-interaction dynamics.

Besides, to promote the clinical use of MRs, proper standards should be established to clarify the priority of MR-based therapeutic platforms over conventional strategies that have already met clinical regulation. Such comparative analyses can ensure the development of MRs well aligns with real clinical needs and requirements, preventing translational failures. We envision that fostering cross-collaboration—spanning clinicians defining clinical needs, engineers developing actuation systems, materials scientists designing MRs, biologists evaluating biosafety, and industry experts addressing scalable manufacturing—will bring fantastic MRs to reality, thereby benefiting both patients and society in the future.

FUNDING AND ACKNOWLEDGMENTS

This work was supported by the National Natural Science Foundation of China with grant nos. 82172335, 81971994, and 91846103; the National Key R&D Program of China with grant no. 2023YFB4705600; the Hong Kong Research Grants Council (RGC) with project nos. STG1/E-401/23-N, RFS2122-4S03, R4015-21, C1134-20GF, 14300621, and 14301122; the National Natural Science Foundation of China with project no. 22102104; Shenzhen Medical Research Fund (SMRF) with grant no. A2303074; Natural Science Foundation of Shenzhen Science and Technology Commission under grants RCBS20200714114920190 and JCYJ20220531103409021; and the Guangdong Basic and Applied Basic Research Foundation with project no. 2021A1515010672. The authors are also grateful for the support from the Multi-scale Medical Robotics Centre (MRC), InnoHK, at the Hong Kong Science Park. The funders had no role in study design, data collection and analysis, decision to publish, or preparation of the manuscript.

AUTHOR CONTRIBUTIONS

Q.W., B.W., X.S., and L.Z. proposed the topic of the review. Q.W. and B.W. wrote the draft. Q.W. edited the figures and tables. Q.W., F.Z., B.W., X.S., L.Z., and J.X. revised the manuscript. K.F.C., B.Y.M.I., and T.W.H.L. contributed to discussions about the review. All authors contributed to the manuscript and approved the final version.

DECLARATION OF INTERESTS

The authors declare no conflicts of interest.

LEAD CONTACT WEBSITE

Li Zhang: http://microbot.mae.cuhk.edu.hk/

REFERENCES

1. Wahlgren, N., Ahmed, N., Dávalos, A. et al. (2007). Thrombolysis with alteplase for acute ischaemic stroke in the Safe Implementation of Thrombolysis in Stroke-Monitoring Study (SITS-MOST): an observational study. *Lancet* **369**:275–282. DOI:https://doi.org/10.1016/S0140-6736(07)60149-4.
2. Emberson, J., Lees, K.R., Lyden, P. et al. (2014). Effect of treatment delay, age, and stroke severity on the effects of intravenous thrombolysis with alteplase for acute ischaemic stroke: a meta-analysis of individual patient data from randomised trials. *Lancet* **384**:1929–1935. DOI:https://doi.org/10.1016/S0140-6736(14)60584-5.
3. Wang, B., Wang, Q., Chan, K.F. et al. (2024). tPA-anchored nanorobots for *in vivo* arterial recanalization at submillimeter-scale segments. *Sci. Adv.* **10**:eadk8970. DOI:https://doi.org/10.1126/sciadv.adk8970.
4. Hortelao, A.C., Simó, C., Guix, M. et al. (2020). Monitoring the collective behavior of enzymatic nanomotors *in vitro* and *in vivo* by PET-CT. Preprint at *bioRxiv*. DOI:https://doi.org/10.1101/2020.06.22.146282.
5. Teasell, R.W., Foley, N.C., Bhogal, S.K. et al. (2003). An evidence-based review of stroke rehabilitation. *Top. Stroke Rehabil.* **10**:29–58. DOI:https://doi.org/10.1310/8YNA-1YHK-YMHB-XTE1.
6. Jolugbo, P. and Ariëns, R.A.S. (2021). Thrombus composition and efficacy of thrombolysis and thrombectomy in acute ischemic stroke. *Stroke* **52**:1131–1142. DOI:https://doi.org/10.1161/STROKEAHA.120.032810.
7. Kasirajan, K., Marek, J.M. and Langsfeld, M. (2001). Mechanical thrombectomy as a first-line treatment for arterial occlusion. *Semin. Vasc. Surg.* **14**:123–131. DOI:https://doi.org/10.1053/svas.2001.23169.
8. Liu, X., Dai, Q., Ye, R. et al. (2020). Endovascular treatment versus standard medical treatment for vertebrobasilar artery occlusion (BEST): an open-label, randomised controlled trial. *Lancet Neurol.* **19**:115–122. DOI:https://doi.org/10.1016/S1474-4422(19)30395-3.
9. Diener, H.-C., Foerch, C., Riess, H. et al. (2013). Treatment of acute ischaemic stroke with thrombolysis or thrombectomy in patients receiving anti-thrombotic treatment. *Lancet Neurol.* **12**:677–688. DOI:https://doi.org/10.1016/S1474-4422(13)70101-7.

10. Bluhmki, E., Chamorro, Á., Dávalos, A. et al. (2009). Stroke treatment with alteplase given 3·0–4·5 h after onset of acute ischaemic stroke (ECASS III): additional outcomes and subgroup analysis of a randomised controlled trial. *Lancet Neurol.* **8**:1095–1102. DOI:https://doi.org/10.1016/S1474-4422(09)70264-9.
11. Nogueira, R.G., Lutsep, H.L., Gupta, R. et al. (2012). Trevo versus Merci retrievers for thrombectomy revascularisation of large vessel occlusions in acute ischaemic stroke (TREVO 2): a randomised trial. *Lancet* **380**:1231–1240. DOI:https://doi.org/10.1016/S0140-6736(12)61299-9.
12. Saver, J.L., Jahan, R., Levy, E.I. et al. (2012). Solitaire flow restoration device versus the Merci Retriever in patients with acute ischaemic stroke (SWIFT): a randomised, parallel-group, non-inferiority trial. *Lancet* **380**:1241–1249. DOI:https://doi.org/10.1016/S0140-6736(12)61384-1.
13. Lapergue, B., Blanc, R., Gory, B. et al. (2017). Effect of endovascular contact aspiration vs stent retriever on revascularization in patients with acute ischemic stroke and large vessel occlusion: the ASTER randomized clinical trial. *JAMA* **318**:443–452. DOI:https://doi.org/10.1001/jama.2017.9644.
14. Rennert, R.C., Wali, A.R., Steinberg, J.A. et al. (2019). Epidemiology, natural history, and clinical presentation of large vessel ischemic stroke. *Neurosurgery* **85**:S4–S8. DOI:https://doi.org/10.1093/neuros/nyz042.
15. Campbell, B.C.V. (2017). Thrombolysis and thrombectomy for acute ischemic stroke: strengths and synergies. *Semin. Thromb. Hemost.* **43**:185–190. DOI:https://doi.org/10.1055/s-0036-1585078.
16. Prabhakaran, S., Ruff, I. and Bernstein, R.A. (2015). Acute stroke intervention: a systematic review. *JAMA* **313**:1451–1462. DOI:https://doi.org/10.1001/jama.2015.3058.
17. van der Worp, H.B. and van Gijn, J. (2007). Acute ischemic stroke. *N. Engl. J. Med.* **357**:572–579. DOI:https://doi.org/10.1056/NEJMcp072057.
18. Wardlaw, J.M., Murray, V., Berge, E. et al. (2012). Recombinant tissue plasminogen activator for acute ischaemic stroke: an updated systematic review and meta-analysis. *Lancet* **379**:2364–2372. DOI:https://doi.org/10.1016/S0140-6736(12)60738-7.
19. Adams, H.P., Jr., del Zoppo, G., Alberts, M.J. et al. (2007). American Heart Association ; American Stroke Association Stroke Council ; Clinical Cardiology Council ; Cardiovascular Radiology and Intervention Council ; Atherosclerotic Peripheral Vascular Disease and Quality of Care Outcomes in Research Interdisciplinary Working Groups. Guidelines for the early management of adults with ischemic stroke : a guideline from the American Heart Association/American Stroke Association Stroke Council, Clinical Cardiology Council, Cardiovascular Radiology and Intervention Council, and the Atherosclerotic Peripheral Vascular Disease and Quality of Care Outcomes in Research Interdisciplinary Working Groups : the American Academy of Neurology affirms the value of this guideline as an educational tool for neurologists. *Stroke* **38**:1655–1711. DOI:https://doi.org/10.1161/STROKEAHA.107.181486.
20. Zoppo, G.J.d., Saver, J.L., Jauch, E.C. et al. (2009). Expansion of the time window for treatment of acute ischemic stroke with intravenous tissue plasminogen activator. *Stroke* **40**:2945–2948. DOI:https://doi.org/10.1161/STROKEAHA.109.192535.
21. Badhiwala, J.H., Nassiri, F., Alhazzani, W. et al. (2015). Endovascular thrombectomy for acute ischemic stroke: a meta-analysis. *JAMA* **314**:1832–1843. DOI:https://doi.org/10.1001/jama.2015.13767.
22. Lansberg, M.G., O'Donnell, M.J., Khatri, P. et al. (2012). Antithrombotic and thrombolytic therapy for ischemic stroke: antithrombotic therapy and prevention of thrombosis, 9th ed: american college of chest physicians evidence-based clinical practice guidelines. *Chest* **141**:e601S–e636S. DOI:https://doi.org/10.1378/chest.11-2302.
23. Tee, J.K., Yip, L.X., Tan, E.S. et al. (2019). Nanoparticles' interactions with vasculature in diseases. *Chem. Soc. Rev.* **48**:5381–5407. DOI:https://doi.org/10.1039/C9CS00309F.
24. Wu, Z., Chen, Y., Mukasa, D. et al. (2020). Medical micro/nanorobots in complex media. *Chem. Soc. Rev.* **49**:8088–8112. DOI:https://doi.org/10.1039/D0CS00309C.
25. Zhang, Y., Yu, J., Bomba, H.N. et al. (2016). Mechanical Force-Triggered Drug Delivery. *Chem. Rev.* **116**:12536–12563. DOI:https://doi.org/10.1021/acs.chemrev.6b00369.
26. Leach, J.K., Patterson, E. and O'Rear, E.A. (2004). Distributed intraclot thrombolysis: mechanism of accelerated thrombolysis with encapsulated plasminogen activators. *J. Thromb. Haemost.* **2**:1548–1555. DOI:https://doi.org/10.1111/j.1538-7836.2004.00884.x.
27. Yang, L., Zhou, Z., Song, J. et al. (2019). Anisotropic nanomaterials for shape-dependent physicochemical and biomedical applications. *Chem. Soc. Rev.* **48**:5140–5176. DOI:https://doi.org/10.1039/C9CS00011A.
28. Chen, J., Wang, L., Xu, H. et al. (2020). Meningeal lymphatics clear erythrocytes that arise from subarachnoid hemorrhage. *Nat. Commun.* **11**:3159. DOI:https://doi.org/10.1038/s41467-020-16851-z.
29. Sitti, M. and Wiersma, D.S. (2020). Pros and cons: magnetic versus optical microrobots. *Adv. Mater.* **32**:1906766. DOI:https://doi.org/10.1002/adma.201906766.
30. Koleoso, M., Feng, X., Xue, Y. et al. (2020). Micro/nanoscale magnetic robots for biomedical applications. *Mater. Today. Bio* **8**:100085. DOI:https://doi.org/10.1016/j.mtbio.2020.100085.
31. Luo, M., Feng, Y., Wang, T. et al. (2018). Micro-/nanorobots at work in active drug delivery. *Adv. Funct. Mater.* **28**:1706100. DOI:https://doi.org/10.1002/adfm.201706100.
32. Soto, F., Wang, J., Ahmed, R. et al. (2020). Medical micro/nanorobots in precision medicine. *Adv. Sci.* **7**:2002203. DOI:https://doi.org/10.1002/advs.202002203.
33. Wang, W. and Zhou, C. (2021). A journey of nanomotors for targeted cancer therapy: principles, challenges, and a critical review of the state-of-the-art. *Adv. Healthc. Mater.* **10**:2001236. DOI:https://doi.org/10.1002/adhm.202001236.
34. Pijpers, I.A.B., Cao, S., Llopis-Lorente, A. et al. (2020). Hybrid biodegradable nanomotors through compartmentalized synthesis. *Nano Lett.* **20**:4472–4480. DOI:https://doi.org/10.1021/acs.nanolett.0c01268.
35. Schmidt, C.K., Medina-Sánchez, M., Edmondson, R.J. et al. (2020). Engineering microrobots for targeted cancer therapies from a medical perspective. *Nat. Commun.* **11**:5618. DOI:https://doi.org/10.1038/s41467-020-19322-7.
36. Gao, C., Wang, Y., Ye, Z. et al. (2021). Biomedical micro-/nanomotors: from overcoming biological barriers to *in vivo* imaging. *Adv. Mater.* **33**:2000512. DOI:https://doi.org/10.1002/adma.202000512.
37. Lowe, G.D.O. (2003). Virchow's triad revisited: abnormal flow. *Pathophysiol. Haemost. Thromb.* **33**:455–457. DOI:https://doi.org/10.1159/000083845.
38. Furie, B. and Furie, B.C. (2008). Mechanisms of thrombus formation. *N. Engl. J. Med.* **359**:938–949. DOI:https://doi.org/10.1056/NEJMra0801082.
39. Zenych, A., Fournier, L. and Chauvierre, C. (2020). Nanomedicine progress in thrombolytic therapy. *Biomaterials* **258**:120297. DOI:https://doi.org/10.1016/j.biomaterials.2020.120297.
40. Stefani, M.A., Schneider, F.L., Marrone, A.C.H. et al. (2013). Influence of the gender on cerebral vascular diameters observed during the magnetic resonance angiographic examination of willis circle. *Braz. Arch. Biol. Technol.* **56**:45–52.
41. Chen, X., Liu, K., Wang, Z. et al. (2015). Computed tomography measurement of pulmonary artery for diagnosis of COPD and its comorbidity pulmonary hypertension. *Int. J. Chron. Obstruct. Pulmon. Dis.* **10**:2525–2533. DOI:https://doi.org/10.2147/COPD.S94211.
42. Felix, U., Salvador Montoya, J., Manuel, D. et al. (1984). Microsurgical anatomy of the proximal segments of the middle cerebral artery. *J. Neurosurg.* **61**:458–467. DOI:https://doi.org/10.3171/jns.1984.61.3.0458.
43. Gabrielsen, T.O. and Greitz, T. (1970). Normal size of the internal carotid, middle cerebral and anterior cerebral arteries. *Acta Radiol. Diagn.* **10**:1–10. DOI:https://doi.org/10.1177/028418517001000101.
44. Bek, S., Kaşikçi, T., Genç, G. et al. (2010). Vasomotor properties of the M2 segment of the middle cerebral artery. *J. Neurol.* **257**:556–562. DOI:https://doi.org/10.1007/s00415-009-5365-2.
45. Krejza, J., Arkuszewski, M., Kasner, S.E. et al. (2006). Carotid artery diameter in men and women and the relation to body and neck size. *Stroke* **37**:1103–1105. DOI:https://doi.org/10.1161/01.STR.0000206440.48756.f7.
46. Zanaty, M., Chalouhi, N., Tjoumakaris, S.I. et al. (2014). Flow-diversion panacea or poison? *Front. Neurol.* **5**:21. DOI:https://doi.org/10.3389/fneur.2014.00021.
47. Ceylan, H., Yasa, I.C., Kilic, U. et al. (2019). Translational prospects of untethered medical microrobots. *Prog. Biomed. Eng.* **1**:012002. DOI:https://doi.org/10.1088/2516-1091/ab22d5.
48. Peyer, K.E., Tottori, S., Qiu, F. et al. (2013). Magnetic helical micromachines. *Chem. Eur J.* **19**:28–38. DOI:https://doi.org/10.1002/chem.201203364.
49. Papaioannou, T.G. and Stefanadis, C. (2005). Vascular wall shear stress: basic principles and methods. *Hellenic J. Cardiol.* **46**:9–15.
50. Korin, N., Gounis, M.J., Wakhloo, A.K. et al. (2015). Targeted drug delivery to flow-obstructed blood vessels using mechanically activated nanotherapeutics. *JAMA Neurol.* **72**:119–122. DOI:https://doi.org/10.1001/jamaneurol.2014.2886.
51. Baylis, J.R., Yeon, J.H., Thomson, M.H. et al. (2015). Self-propelled particles that transport cargo through flowing blood and halt hemorrhage. *Sci. Adv.* **1**:e1500379. DOI:https://doi.org/10.1126/sciadv.1500379.
52. Alapan, Y., Bozuyuk, U., Erkoc, P. et al. (2020). Multifunctional surface microrollers for targeted cargo delivery in physiological blood flow. *Sci. Robot.* **5**:eaba5726. DOI:https://doi.org/10.1126/scirobotics.aba5726.
53. Wang, Q., Chan, K.F., Schweizer, K. et al. (2021). Ultrasound Doppler-guided real-time navigation of a magnetic microswarm for active endovascular delivery. *Sci. Adv.* **7**:eabe5914. DOI:https://doi.org/10.1126/sciadv.abe5914.
54. De Jong, W.H. and Borm, P.J.A. (2008). Drug delivery and nanoparticles: applications and hazards. *Int. J. Nanomedicine* **3**:133–149. DOI:https://doi.org/10.2147/ijn.s596.
55. Li, S.-D. and Huang, L. (2008). Pharmacokinetics and biodistribution of nanoparticles. *Mol. Pharm.* **5**:496–504. DOI:https://doi.org/10.1021/mp800049w.
56. Zheng, J., Qi, R., Dai, C. et al. (2022). Enzyme catalysis biomotor engineering of neutrophils for nanodrug delivery and cell-based thrombolytic therapy. *ACS Nano.* **16**:2330–2344. DOI:https://doi.org/10.1021/acsnano.1c08538.
57. Wan, M., Wang, Q., Wang, R. et al. (2020). Platelet-derived porous nanomotor for thrombus therapy. *Sci. Adv.* **6**:eaaz9014. DOI:https://doi.org/10.1126/sciadv.aaz9014.
58. Nelson, B.J. and Pané, S. (2023). Delivering drugs with microrobots. *Science* **382**:1120–1122. DOI:https://doi.org/10.1126/science.adh3073.
59. Wang, B., Kostarelos, K., Nelson, B.J. et al. (2021). Trends in micro-/nanorobotics: materials development, actuation, localization, and system integration for biomedical applications. *Adv. Mater.* **33**:2002047. DOI:https://doi.org/10.1002/adma.202002047.
60. Wang, J., Dong, Y., Ma, P. et al. (2022). Intelligent micro-/nanorobots for cancer theragnostic. *Adv. Mater.* **34**:2201051. DOI:https://doi.org/10.1002/adma.202201051.
61. Mayorga-Martinez, C.C., Zhang, L. and Pumera, M. (2024). Chemical multiscale robotics for bacterial biofilm treatment. *Chem. Soc. Rev.* **53**:2284–2299. DOI:https://doi.org/10.1039/D3CS00564J.
62. Del Campo Fonseca, A., Glück, C., Droux, J. et al. (2023). Ultrasound trapping and navigation of microrobots in the mouse brain vasculature. *Nat. Commun.* **14**:5889. DOI:https://doi.org/10.1038/s41467-023-41557-3.
63. Wang, Q., Du, X., Jin, D. et al. (2022). Real-time ultrasound Doppler tracking and autonomous navigation of a miniature helical robot for accelerating thrombolysis in dynamic blood flow. *ACS Nano.* **16**:604–616. DOI:https://doi.org/10.1021/acsnano.1c07830.
64. Zhang, F., Zhuang, J., Li, Z. et al. (2022). Nanoparticle-modified microrobots for *in vivo* antibiotic delivery to treat acute bacterial pneumonia. *Nat. Mater.* **21**:1324–1332. DOI:https://doi.org/10.1038/s41563-022-01360-9.

65. Liu, L., Li, S., Yang, K. et al. (2023). Drug-free antimicrobial nanomotor for precise treatment of multidrug-resistant bacterial infections. *Nano Lett.* **23**:3929–3938. DOI:https://doi.org/10.1021/acs.nanolett.3c00632.
66. Sánchez, S., Soler, L. and Katuri, J. (2015). Chemically powered micro- and nanomotors. *Angew. Chem. Int. Ed.* **54**:1414–1444. DOI:https://doi.org/10.1002/anie.201406096.
67. Guix, M., Mayorga-Martinez, C.C. and Merkoçi, A. (2014). Nano/micromotors in (bio)chemical science applications. *Chem. Rev.* **114**:6285–6322. DOI:https://doi.org/10.1021/cr400273r.
68. Lyu, Z., Yao, L., Wang, Z. et al. (2024). Nanoscopic imaging of self-propelled ultrasmall catalytic nanomotors. *ACS Nano.* **18**:14231–14243. DOI:https://doi.org/10.1021/acsnano.3c12590.
69. Brooks, A.M., Tasinkevych, M., Sabrina, S. et al. (2019). Shape-directed rotation of homogeneous micromotors via catalytic self-electrophoresis. *Nat. Commun.* **10**:495. DOI:https://doi.org/10.1038/s41467-019-08423-7.
70. Zhan, X., Wang, J., Xiong, Z. et al. (2019). Enhanced ion tolerance of electrokinetic locomotion in polyelectrolyte-coated microswimmer. *Nat. Commun.* **10**:3921. DOI:https://doi.org/10.1038/s41467-019-11907-1.
71. Wang, J., Xiong, Z., Zheng, J. et al. (2018). Light-driven micro/nanomotor for promising biomedical tools: principle, challenge, and prospect. *Acc. Chem. Res.* **51**:1957–1965. DOI:https://doi.org/10.1021/acs.accounts.8b00254.
72. Xu, L., Mou, F., Gong, H. et al. (2017). Light-driven micro/nanomotors: from fundamentals to applications. *Chem. Soc. Rev.* **46**:6905–6926. DOI:https://doi.org/10.1039/C7CS00516D.
73. Maric, T., Løvind, A., Zhang, Z. et al. (2023). Near-infrared light-driven mesoporous SiO_2/AU nanomotors for eradication of pseudomonas aeruginosa biofilm. *Adv. Healthc. Mater.* **12**:2203018. DOI:https://doi.org/10.1002/adhm.202203018.
74. Hu, Z., Tan, H., Ye, Y. et al. (2024). NIR-actuated ferroptosis nanomotor for enhanced tumor penetration and therapy. *Adv. Mater.* **36**:2412227. DOI:https://doi.org/10.1002/adma.202412227.
75. Shao, J., Abdelghani, M., Shen, G. et al. (2018). Erythrocyte membrane modified Janus polymeric motors for thrombus therapy. *ACS Nano.* **12**:4877–4885. DOI:https://doi.org/10.1021/acsnano.8b01772.
76. Han, H., Ma, X., Deng, W. et al. (2024). Imaging-guided bioresorbable acoustic hydrogel microrobots. *Sci. Robot.* **9**:eadp3593. DOI:https://doi.org/10.1126/scirobotics.adp3593.
77. Aghakhani, A., Pena-Francesch, A., Bozuyuk, U. et al. (2022). High shear rate propulsion of acoustic microrobots in complex biological fluids. *Sci. Adv.* **8**:eabm5126. DOI:https://doi.org/10.1126/sciadv.abm5126.
78. Zhu, S., Chen, Y., Liu, G. et al. (2022). External field-driven untethered microrobots for targeted cargo delivery. *Adv. Mat. Tech.* **7**:2101256. DOI:https://doi.org/10.1002/admt.202101256.
79. Zhang, F., Guo, Z., Li, Z. et al. (2024). Biohybrid microrobots locally and actively deliver drug-loaded nanoparticles to inhibit the progression of lung metastasis. *Sci. Adv.* **10**:eadn6157. DOI:https://doi.org/10.1126/sciadv.adn6157.
80. Alvarez, L., Friedrich, B.M., Gompper, G. et al. (2014). The computational sperm cell. *Trends Cell Biol.* **24**:198–207. DOI:https://doi.org/10.1016/j.tcb.2013.10.004.
81. Jin, D., Yuan, K., Du, X. et al. (2021). Domino reaction encoded heterogeneous colloidal microswarm with on-demand morphological adaptability. *Adv. Mater.* **33**:2100070. DOI:https://doi.org/10.1002/adma.202100070.
82. Sun, M., Chan, K.F., Zhang, Z. et al. (2022). Magnetic microswarm and fluoroscopy-guided platform for biofilm eradication in biliary stents. *Adv. Mater.* **34**:2201888. DOI:https://doi.org/10.1002/adma.202201888.
83. Yu, J., Jin, D., Chan, K.-F. et al. (2019). Active generation and magnetic actuation of microrobotic swarms in bio-fluids. *Nat. Commun.* **10**:5631. DOI:https://doi.org/10.1038/s41467-019-13576-6.
84. Zhou, H., Mayorga-Martinez, C.C., Pané, S. et al. (2021). Magnetically driven micro and nanorobots. *Chem. Rev.* **121**:4999–5041. DOI:https://doi.org/10.1021/acs.chemrev.0c01234.
85. Dong, Y., Wang, L., Iacovacci, V. et al. (2022). Magnetic helical micro-/nanomachines: recent progress and perspective. *Matter* **5**:77–109. DOI:https://doi.org/10.1016/j.matt.2021.10.010.
86. Tottori, S., Zhang, L., Qiu, F. et al. (2012). Magnetic helical micromachines: fabrication, controlled swimming, and cargo transport. *Adv. Mater.* **24**:811–816. DOI:https://doi.org/10.1002/adma.201103818.
87. Wang, M., Wu, T., Liu, R. et al. (2023). Selective and independent control of microrobots in a magnetic field: a review. *Engineering* **24**:21–38. DOI:https://doi.org/10.1016/j.eng.2023.02.011.
88. Jeong, S., Choi, H., Cha, K. et al. (2011). Enhanced locomotive and drilling microrobot using precessional and gradient magnetic field. *Sens. Actuators A: Phys.* **171**:429–435. DOI:https://doi.org/10.1016/j.sna.2011.08.020.
89. Yang, L., Yu, J., Yang, S. et al. (2022). A survey on swarm microrobotics. *IEEE Trans. Robot.* **38**:1531–1551. DOI:https://doi.org/10.1109/TRO.2021.3111788.
90. Servant, A., Qiu, F., Mazza, M. et al. (2015). Controlled *in vivo* swimming of a swarm of bacteria-like microrobotic flagella. *Adv. Mater.* **27**:2981–2988. DOI:https://doi.org/10.1002/adma.201404444.
91. Jin, D. and Zhang, L. (2022). Collective behaviors of magnetic active matter: recent progress toward reconfigurable, adaptive, and multifunctional swarming micro/nanorobots. *Acc. Chem. Res.* **55**:98–109. DOI:https://doi.org/10.1021/acs.accounts.1c00619.
92. Medina-Sánchez, M. and Schmidt, O.G. (2017). Medical microbots need better imaging and control. *Nature* **545**:406–408. DOI:https://doi.org/10.1038/545406a.
93. Agrahari, V., Agrahari, V., Chou, M.-L. et al. (2020). Intelligent micro-/nanorobots as drug and cell carrier devices for biomedical therapeutic advancement: promising development opportunities and translational challenges. *Biomaterials* **260**:120163. DOI:https://doi.org/10.1016/j.biomaterials.2020.120163.
94. Liu, W., Liu, Y., Li, H. et al. (2023). Biomedical micro-/nanomotors: design, imaging, and disease treatment. *Adv. Funct. Mater.* **33**:2212452. DOI:https://doi.org/10.1002/adfm.202212452.
95. Zhang, H., Li, Z., Gao, C. et al. (2021). Dual-responsive biohybrid neutrobots for active target delivery. *Sci. Robot.* **6**:eaaz9519. DOI:https://doi.org/10.1126/scirobotics.aaz9519.
96. Wrede, P., Degtyaruk, O., Kalva, S.K. et al. (2022). Real-time 3D optoacoustic tracking of cell-sized magnetic microrobots circulating in the mouse brain vasculature. *Sci. Adv.* **8**:eabm9132. DOI:https://doi.org/10.1126/sciadv.abm9132.
97. Wang, Q., Wang, Q., Ning, Z. et al. (2024). Tracking and navigation of a microswarm under laser speckle contrast imaging for targeted delivery. *Sci. Robot.* **9**:eadh1978. DOI:https://doi.org/10.1126/scirobotics.adh1978.
98. Go, G., Yoo, A., Nguyen, K.T. et al. (2022). Multifunctional microrobot with real-time visualization and magnetic resonance imaging for chemoembolization therapy of liver cancer. *Sci. Adv.* **8**:eabq8545. DOI:https://doi.org/10.1126/sciadv.abq8545.
99. Mhanna, R., Qiu, F., Zhang, L. et al. (2014). Artificial bacterial flagella for remote-controlled targeted single-cell drug delivery. *Small* **10**:1953–1957. DOI:https://doi.org/10.1002/smll.201303538.
100. Steager, E.B., Selman, S.M., Magee, C. et al. (2013). Automated biomanipulation of single cells using magnetic microrobots. *Int. J. Robot Res.* **32**:346–359. DOI:https://doi.org/10.1177/0278364912472381.
101. Sánchez, A., Magdanz, V., Schmidt, O.G. et al. (2014). Magnetic control of self-propelled microjets under ultrasound image guidance. In 5th IEEE RAS/EMBS International Conference on Biomedical Robotics and Biomechatronics, pp. 169–174. DOI:https://doi.org/10.1109/BIOROB.2014.6913771.
102. Olson, E.S., Orozco, J., Wu, Z. et al. (2013). Toward *in vivo* detection of hydrogen peroxide with ultrasound molecular imaging. *Biomaterials* **34**:8918–8924. DOI:https://doi.org/10.1016/j.biomaterials.2013.06.055.
103. Martel, S., Mathieu, J.-B., Felfoul, O. et al. (2007). Automatic navigation of an untethered device in the artery of a living animal using a conventional clinical magnetic resonance imaging system. *Appl. Phys. Lett.* **90**:114105. DOI:https://doi.org/10.1063/1.2713229.
104. Mathieu, J.B., Beaudoin, G. and Martel, S. (2006). Method of propulsion of a ferromagnetic core in the cardiovascular system through magnetic gradients generated by an MRI system. *IEEE Trans. Biomed. Eng.* **53**:292–299. DOI:https://doi.org/10.1109/TBME.2005.862570.
105. Yan, X., Zhou, Q., Vincent, M. et al. (2017). Multifunctional biohybrid magnetite microrobots for imaging-guided therapy. *Sci. Robot.* **2**:eaaq1155. DOI:https://doi.org/10.1126/scirobotics.aaq1155.
106. Vilela, D., Cossío, U., Parmar, J. et al. (2018). Medical imaging for the tracking of micromotors. *ACS Nano.* **12**:1220–1227. DOI:https://doi.org/10.1021/acsnano.7b07220.
107. Xie, L., Pang, X., Yan, X. et al. (2020). Photoacoustic imaging-trackable magnetic microswimmers for pathogenic bacterial infection treatment. *ACS Nano.* **14**:2880–2893. DOI:https://doi.org/10.1021/acsnano.9b06731.
108. Kherlopian, A.R., Song, T., Duan, Q. et al. (2008). A review of imaging techniques for systems biology. *BMC Syst. Biol.* **2**:74. DOI:https://doi.org/10.1186/1752-0509-2-74.
109. Lu, F.-M. and Yuan, Z. (2015). PET/SPECT molecular imaging in clinical neuroscience: recent advances in the investigation of CNS diseases. *Quant. Imaging Med. Surg.* **5**:433–447. DOI:https://doi.org/10.3978/j.issn.2223-4292.2015.03.16.
110. Panés, J., Bouzas, R., Chaparro, M. et al. (2011). Systematic review: the use of ultrasonography, computed tomography and magnetic resonance imaging for the diagnosis, assessment of activity and abdominal complications of Crohn's disease. *Aliment. Pharmacol. Ther.* **34**:125–145. DOI:https://doi.org/10.1111/j.1365-2036.2011.04710.x.
111. Aaron, F., A, F. and Downey, D.B. (2000). Three-dimensional ultrasound imaging. *Annu. Rev. Biomed. Eng.* **2**:457–475. DOI:https://doi.org/10.1146/annurev.bioeng.2.1.457.
112. Aziz, A., Pane, S., Iacovacci, V. et al. (2020). Medical imaging of microrobots: toward *in vivo* applications. *ACS Nano.* **14**:10865–10893. DOI:https://doi.org/10.1021/acsnano.0c05530.
113. Ren, E., Hu, J., Mei, Z. et al. (2025). Water-stable magnetic lipiodol micro-droplets as a miniaturized robotic tool for drug delivery. *Adv. Mater.* **37**:2412187. DOI:https://doi.org/10.1002/adma.202412187.
114. Jin, D., Wang, Q., Chan, K.F. et al. (2023). Swarming self-adhesive microgels enabled aneurysm on-demand embolization in physiological blood flow. *Sci. Adv.* **9**:eadf9278. DOI:https://doi.org/10.1126/sciadv.adf9278.
115. Liu, X., Wang, L., Xiang, Y. et al. (2024). Magnetic soft microfiberbots for robotic embolization. *Sci. Robot.* **9**:eadh2479. DOI:https://doi.org/10.1126/scirobotics.adh2479.
116. Jeong, S., Choi, H., Go, G. et al. (2016). Penetration of an artificial arterial thromboembolism in a live animal using an intravascular therapeutic microrobot system. *Med. Eng. Phys.* **38**:403–410. DOI:https://doi.org/10.1016/j.medengphy.2016.01.001.
117. de Ávila, B.E.F., Angsantikul, P., Li, J. et al. (2017). Micromotor-enabled active drug delivery for *in vivo* treatment of stomach infection. *Nat. Commun.* **8**:272. DOI:https://doi.org/10.1038/s41467-017-00309-w.
118. Zhang, Z., Yan, H., Li, S. et al. (2021). Janus rod-like micromotors to promote the tumor accumulation and cell internalization of therapeutic agents. *Chem. Eng. J.* **404**:127073. DOI:https://doi.org/10.1016/j.cej.2020.127073.
119. Wang, D., Han, X., Dong, B. et al. (2021). Stimuli responsiveness, propulsion and application of the stimuli-responsive polymer based micromotor. *Appl. Mater. Today* **25**:101250. DOI:https://doi.org/10.1016/j.apmt.2021.101250.

120. Luan, J., Kuijken, P.F., Chen, W. et al. (2023). Microfluidic design of streamlined alginate hydrogel micromotors with run and tumble motion patterns. *Adv. Sci.* **10**:2304995. DOI:https://doi.org/10.1002/advs.202304995.
121. Karshalev, E., Esteban-Fernández de Ávila, B., Beltrán-Gastélum, M. et al. (2018). Micromotor pills as a dynamic oral delivery platform. *ACS Nano.* **12**:8397–8405. DOI:https://doi.org/10.1021/acsnano.8b03760.
122. Zhang, F., Mundaca-Uribe, R., Askarinam, N. et al. (2022). Biomembrane-functionalized micromotors: biocompatible active devices for diverse biomedical applications. *Adv. Mater.* **34**:2107177. DOI:https://doi.org/10.1002/adma.202107177.
123. Xu, C., Wang, S., Wang, H. et al. (2021). Magnesium-based micromotors as hydrogen generators for precise rheumatoid arthritis therapy. *Nano Lett.* **21**:1982–1991. DOI:https://doi.org/10.1021/acs.nanolett.0c04438.
124. Gao, W., Pei, A. and Wang, J. (2012). Water-driven micromotors. *ACS Nano.* **6**:8432–8438. DOI:https://doi.org/10.1021/nn303309z.
125. Ye, J., Fu, Q., Liu, L. et al. (2021). Ultrasound-propelled Janus Au NR-mSiO_2 nanomotor for NIR-II photoacoustic imaging guided sonodynamic-gas therapy of large tumors. *Sci. China Chem.* **64**:2218–2229. DOI:https://doi.org/10.1007/s11426-021-1070-6.
126. Jang, B., Hong, A., Kang, H.E. et al. (2017). Multiwavelength light-responsive Au/B-TiO_2 Janus micromotors. *ACS Nano.* **11**:6146–6154. DOI:https://doi.org/10.1021/acsnano.7b02177.
127. Zhang, Y., Zhang, L., Yang, L. et al. (2019). Real-time tracking of fluorescent magnetic spore-based microrobots for remote detection of C. diff toxins. *Sci. Adv.* **5**:eaau9650. DOI:https://doi.org/10.1126/sciadv.aau9650.
128. Ou, J., Tian, H., Wu, J. et al. (2021). MnO_2-based nanomotors with active Fenton-like Mn^{2+} delivery for enhanced chemodynamic therapy. *ACS Appl. Mater. Inter.* **13**:38050–38060. DOI:https://doi.org/10.1021/acsami.1c08926.
129. Zhang, H., Cao, Z., Zhang, Q. et al. (2020). Chemotaxis-driven 2D nanosheet for directional drug delivery toward the tumor microenvironment. *Small* **16**:2002732. DOI:https://doi.org/10.1002/smll.202002732.
130. Wu, Z., Troll, J., Jeong, H.-H. et al. (2018). A swarm of slippery micropropellers penetrates the vitreous body of the eye. *Sci. Adv.* **4**:eaat4388. DOI:https://doi.org/10.1126/sciadv.aat4388.
131. Su, L., Jin, D., Wang, Y. et al. (2023). Modularized microrobot with lock-and-detachable modules for targeted cell delivery in bile duct. *Sci. Adv.* **9**:eadj0883. DOI:https://doi.org/10.1126/sciadv.adj0883.
132. Iacovacci, V., Ricotti, L., Sinibaldi, E. et al. (2018). An intravascular magnetic catheter enables the retrieval of nanoagents from the bloodstream. *Adv. Sci.* **5**:1800807. DOI:https://doi.org/10.1002/advs.201800807.
133. Xie, M., Zhang, W., Fan, C. et al. (2020). Bioinspired soft microrobots with precise magneto-collective control for microvascular thrombolysis. *Adv. Mater.* **32**:2000366. DOI:https://doi.org/10.1002/adma.202000366.
134. Kim, Y. and Zhao, X. (2022). Magnetic soft materials and robots. *Chem. Rev.* **122**:5317–5364. DOI:https://doi.org/10.1021/acs.chemrev.1c00481.
135. Theato, P., Sumerlin, B.S., O'Reilly, R.K. et al. (2013). Stimuli responsive materials. *Chem. Soc. Rev.* **42**:7055–7056. DOI:https://doi.org/10.1039/C3CS90057F.
136. Municoy, S., Álvarez Echazú, M.I., Antezana, P.E. et al. (2020). Stimuli-responsive materials for tissue engineering and drug delivery. *Int. J. Mol. Sci.* **21**:4724. DOI:https://doi.org/10.3390/ijms21134724.
137. Cedervall, T., Lynch, I., Lindman, S. et al. (2007). Understanding the nanoparticle–protein corona using methods to quantify exchange rates and affinities of proteins for nanoparticles. *Proc. Natl. Acad. Sci. USA* **104**:2050–2055. DOI:https://doi.org/10.1073/pnas.0608582104.
138. Pino, P.d., Pelaz, B., Zhang, Q. et al. (2014). Protein corona formation around nanoparticles–from the past to the future. *Mater. Horiz.* **1**:301–313. DOI:https://doi.org/10.1039/C3MH00106G.
139. Pederzoli, F., Tosi, G., Vandelli, M.A. et al. (2017). Protein corona and nanoparticles: how can we investigate on? *WIREs Nanomed. Nanobiotechnol.* **9**:e1467. DOI:https://doi.org/10.1002/wnan.1467.
140. Barz, M., Parak, W.J. and Zentel, R. (2024). Concepts and approaches to reduce or avoid protein corona formation on nanoparticles: challenges and opportunities. *Adv. Sci.* **11**:2402935. DOI:https://doi.org/10.1002/advs.202402935.
141. Mahmoudi, M., Landry, M.P., Moore, A. et al. (2023). The protein corona from nanomedicine to environmental science. *Nat. Rev. Mater.* **8**:1–17. DOI:https://doi.org/10.1038/s41578-023-00552-2.
142. Hosney, A., Abdalla, J., Amin, I.S. et al. (2016). In vitro validation of clearing clogged vessels using microrobots. In 2016 6th IEEE International Conference on Biomedical Robotics and Biomechatronics (BioRob) (IEEE), pp. 272–277. DOI:https://doi.org/10.1109/BIOROB.2016.7523637.
143. Xue, C., Zhan, J. and Li, X. (2016). Thrombus clean-up with magneto-elastic μ-vibrator. In 2016 IEEE 29th International Conference on Micro Electro Mechanical Systems (MEMS) (IEEE), pp. 415–418. DOI:https://doi.org/10.1109/MEMSYS.2016.7421649.
144. Khalil, I.S.M., Tabak, A.F., Sadek, K. et al. (2017). Rubbing against blood clots using helical robots: modeling and *in vitro* experimental validation. *IEEE Robot. Autom. Lett.* **2**:927–934. DOI:https://doi.org/10.1109/LRA.2017.2654546.
145. Lee, S., Lee, S., Kim, S. et al. (2018). Fabrication and characterization of a magnetic drilling actuator for navigation in a three-dimensional phantom vascular network. *Sci. Rep.* **8**:3691. DOI:https://doi.org/10.1038/s41598-018-22110-5.
146. Khalil, I.S.M., Mahdy, D., Sharkawy, A.E. et al. (2018). Mechanical rubbing of blood clots using helical robots under ultrasound guidance. *IEEE Robot. Autom. Lett.* **3**:1112–1119. DOI:https://doi.org/10.1109/LRA.2018.2792156.
147. Khalil, I.S.M., Adel, A., Mahdy, D. et al. (2019). Magnetic localization and control of helical robots for clearing superficial blood clots. *APL Bioeng.* **3**:026104. DOI:https://doi.org/10.1063/1.5090872.
148. Leclerc, J., Zhao, H., Bao, D. et al. (2020). In vitro design investigation of a rotating helical magnetic swimmer for combined 3-D navigation and blood clot removal. *IEEE Trans. Robot.* **36**:975–982. DOI:https://doi.org/10.1109/TRO.2020.2988636.
149. Cheng, R., Huang, W., Huang, L. et al. (2014). Acceleration of tissue plasminogen activator-mediated thrombolysis by magnetically powered nanomotors. *ACS Nano.* **8**:7746–7754. DOI:https://doi.org/10.1021/nn5029955.
150. Hu, J., Huang, W., Huang, S. et al. (2016). Magnetically active Fe_3O_4 nanorods loaded with tissue plasminogen activator for enhanced thrombolysis. *Nano Res.* **9**:2652–2661. DOI:https://doi.org/10.1007/s12274-016-1152-4.
151. Tasci, T.O., Disharoon, D., Schoeman, R.M. et al. (2017). Enhanced fibrinolysis with magnetically powered colloidal microwheels. *Small* **13**:1700954. DOI:https://doi.org/10.1002/smll.201700954.
152. Hu, J., Huang, S., Zhu, L. et al. (2018). Tissue plasminogen activator-porous magnetic microrods for targeted thrombolytic therapy after ischemic stroke. *ACS Appl. Mater. Inter.* **10**:32988–32997. DOI:https://doi.org/10.1021/acsami.8b09423.
153. Cao, W., Liu, Y., Ran, P. et al. (2021). Ultrasound-propelled Janus rod-shaped micromotors for site-specific sonodynamic thrombolysis. *ACS Appl. Mater. Inter.* **13**:58411–58421. DOI:https://doi.org/10.1021/acsami.1c19288.
154. Wang, Q., Wang, B., Yu, J. et al. (2020). Reconfigurable magnetic microswarm for thrombolysis under ultrasound imaging. In 2020 IEEE International Conference on Robotics and Automation (ICRA) (IEEE), pp. 10285–10291. DOI:https://doi.org/10.1109/ICRA40945.2020.9197432.
155. Wang, L., Wang, J., Hao, J. et al. (2021). Guiding drug through interrupted bloodstream for potentiated thrombolysis by C-shaped magnetic actuation system *in vivo*. *Adv. Mater.* **33**:2105351. DOI:https://doi.org/10.1002/adma.202105351.
156. Tang, X., Manamanchaiyaporn, L., Zhou, Q. et al. (2022). Synergistic integration and pharmacomechanical function of enzyme-magnetite nanoparticle swarms for low-dose fast thrombolysis. *Small* **18**:2202848. DOI:https://doi.org/10.1002/smll.202202848.
157. Xie, S., Li, S., Cao, W. et al. (2022). Bacteria-templated and dual enzyme-powered microcapsule motors to promote thrombus penetration and thrombolytic efficacy. *ACS Appl. Mater. Inter.* **14**:37553–37565. DOI:https://doi.org/10.1021/acsami.2c11213.
158. Yang, M., Zhang, Y., Mou, F. et al. (2023). Swarming magnetic nanorobots bio-interfaced by heparinoid-polymer brushes for *in vivo* safe synergistic thrombolysis. *Sci. Adv.* **9**:eadk7251. DOI:https://doi.org/10.1126/sciadv.adk7251.
159. Dogangil, G., Ergeneman, O., Abbott, J.J. et al. (2008). Toward targeted retinal drug delivery with wireless magnetic microrobots. In 2008 IEEE/RSJ International Conference on Intelligent Robots and Systems (IEEE), pp. 1921–1926. DOI:https://doi.org/10.1109/IROS.2008.4650768.
160. Jang, G.B., Jeon, S., Nam, J. et al. (2015). A spiral microrobot performing navigating linear and drilling motions by magnetic gradient and rotating uniform magnetic field for applications in unclogging blocked human blood vessels. *IEEE Trans. Magn.* **51**:1–4. DOI:https://doi.org/10.1109/TMAG.2015.2436913.
161. Yu, C., Kim, J., Choi, H. et al. (2010). Novel electromagnetic actuation system for three-dimensional locomotion and drilling of intravascular microrobot. *Sens. Actuators A: Phys.* **161**:297–304. DOI:https://doi.org/10.1016/j.sna.2010.04.037.
162. Choi, H., Cha, K., Jeong, S. et al. (2013). 3-D locomotive and drilling microrobot using novel stationary EMA system. *IEEE ASME Trans. Mechatron.* **18**:1221–1225. DOI:https://doi.org/10.1109/TMECH.2012.2201494.
163. Lee, W., Jeon, S., Nam, J. et al. (2015). Dual-body magnetic helical robot for drilling and cargo delivery in human blood vessels. *J. Appl. Phys.* **117**:17B314. DOI:https://doi.org/10.1063/1.4917067.
164. Go, G., Choi, H., Jeong, S. et al. (2015). Electromagnetic navigation system using simple coil structure (4 coils) for 3-D locomotive microrobot. *IEEE Trans. Mag* **51**:1–7. DOI:https://doi.org/10.1109/TMAG.2014.2364543.
165. Yang, Z. and Zhang, L. (2020). Magnetic actuation systems for miniature robots: a review. *Adv. Intell. Syst.* **2**:2000082. DOI:https://doi.org/10.1002/aisy.202000082.
166. Xu, L., Luo, Y., Du, Q. et al. (2023). Magnetic response combined with bioactive ion therapy: a RONS-scavenging theranostic nanoplatform for thrombolysis and renal ischemia–reperfusion injury. *ACS Nano.* **17**:5695–5712. DOI:https://doi.org/10.1021/acsnano.2c12091.
167. Li, S., Gu, H.-Q., Li, H. et al. (2024). Reteplase versus alteplase for acute ischemic stroke. *N. Engl. J. Med.* **390**:2264–2273. DOI:https://doi.org/10.1056/NEJMoa2400314.
168. Andersen, J.K. (2004). Oxidative stress in neurodegeneration: cause or consequence? *Nat. Med.* **10**:S18–S25. DOI:https://doi.org/10.1038/nrn1434.
169. Kanazawa, M., Takahashi, T., Nishizawa, M. et al. (2017). Therapeutic strategies to attenuate hemorrhagic transformation after tissue plasminogen activator treatment for acute ischemic stroke. *J. Atheroscler. Thromb.* **24**:240–253. DOI:https://doi.org/10.5551/jat.RV16006.
170. Quan, X., Liang, X., Ding, Y. et al. (2023). Cryo-shocked platelet coupled with ROS-responsive nanomedicine for targeted treatment of thromboembolic disease. *ACS Nano.* **17**:6519–6533. DOI:https://doi.org/10.1021/acsnano.2c11865.
171. Cheng, J., Zhang, S., Li, C. et al. (2022). Functionally integrating nanoparticles alleviate deep vein thrombosis in pregnancy and rescue intrauterine growth restriction. *Nat. Commun.* **13**:7166. DOI:https://doi.org/10.1038/s41467-022-34878-2.
172. Nemoto, E.M. and Frinak, S. (1981). Brain tissue pH after global brain ischemia and barbiturate loading in rats. *Stroke* **12**:77–82. DOI:https://doi.org/10.1161/01.STR.12.1.77.

173. Mei, T., Kim, A., Vong, L.B. et al. (2019). Encapsulation of tissue plasminogen activator in pH-sensitive self-assembled antioxidant nanoparticles for ischemic stroke treatment – Synergistic effect of thrombolysis and antioxidant. *Biomaterials* **215**:119209. DOI:https://doi.org/10.1016/j.biomaterials.2019.05.020.
174. Bark, D.L. and Ku, D.N. (2010). Wall shear over high degree stenoses pertinent to atherothrombosis. *J. Biomech.* **43**:2970–2977. DOI:https://doi.org/10.1016/j.jbiomech.2010.07.011.
175. Korin, N., Kanapathipillai, M., Matthews, B.D. et al. (2012). Shear-activated nanotherapeutics for drug targeting to obstructed blood vessels. *Science* **337**:738–742. DOI:https://doi.org/10.1126/science.1217815.
176. Xu, X., Huang, X., Zhang, Y. et al. (2020). Self-regulated hirudin delivery for anticoagulant therapy. *Sci. Adv.* **6**:eabc0382. DOI:https://doi.org/10.1126/sciadv.abc0382.
177. Zhang, H., Zhao, Z., Sun, S. et al. (2023). Molecularly self-fueled nano-penetrator for non-pharmaceutical treatment of thrombosis and ischemic stroke. *Nat. Commun.* **14**:255. DOI:https://doi.org/10.1038/s41467-023-35895-5.
178. Silvennoinen, H.M., Ikonen, S., Soinne, L. et al. (2007). CT angiographic analysis of carotid artery stenosis: comparison of manual assessment, semiautomatic vessel analysis, and digital subtraction angiography. *Am. J. Neuroradiol.* **28**:97–103.
179. Bladin, C., Levi, C., Parsons, M. et al. (2015). Abstract 187: magnetically-enhanced diffusion (MED) of intravenous tPA in acute ischemic stroke: a pilot safety and feasibility trial. *Stroke* **46**:A187. DOI:https://doi.org/10.1161/str.46.suppl_1.187.
180. Dreyfus, R., Boehler, Q., Lyttle, S. et al. (2024). Dexterous helical magnetic robot for improved endovascular access. *Sci. Robot.* **9**:eadh0298. DOI:https://doi.org/10.1126/scirobotics.adh0298.
181. Kim, Y., Genevriere, E., Harker, P. et al. (2022). Telerobotic neurovascular interventions with magnetic manipulation. *Sci. Robot.* **7**:eabg9907. DOI:https://doi.org/10.1126/scirobotics.abg9907.
182. Yang, L., Jiang, J., Gao, X. et al. (2022). Autonomous environment-adaptive microrobot swarm navigation enabled by deep learning-based real-time distribution planning. *Nat. Mach. Intell.* **4**:480–493. DOI:https://doi.org/10.1038/s42256-022-00482-8.
183. Abbasi, S.A., Ahmed, A., Noh, S. et al. (2024). Autonomous 3D positional control of a magnetic microrobot using reinforcement learning. *Nat. Mach. Intell.* **6**:92–105. DOI:https://doi.org/10.1038/s42256-023-00779-2.
184. Panayides, A.S., Amini, A., Filipovic, N.D. et al. (2020). AI in medical imaging informatics: current challenges and future directions. *IEEE J. Biomed. Health Inform.* **24**:1837–1857. DOI:https://doi.org/10.1109/JBHI.2020.2991043.
185. Yang, L., Jiang, J., Ji, F. et al. (2024). Machine learning for micro- and nanorobots. *Nat. Mach. Intell.* **6**:605–618. DOI:https://doi.org/10.1038/s42256-024-00859-x.
186. ROY, K., GOMEZ-PULIDO, F. and ERNST, S. (2016). Remote magnetic navigation for catheter ablation in patients with congenital heart disease: a review. *J. Cardiovasc. Electrophysiol.* **27**:S45–S56. DOI:https://doi.org/10.1111/jce.12903.
187. Faddis, M.N., Blume, W., Finney, J. et al. (2002). Novel, magnetically guided catheter for endocardial mapping and radiofrequency catheter ablation. *Circulation* **106**:2980–2985. DOI:https://doi.org/10.1161/01.CIR.0000038704.84304.6F.
188. Liu, J., Wang, Q., Wang, H. et al. (2016). Design and fabrication of a catheter magnetic navigation system for cardiac arrhythmias. *IEEE Trans. Appl. Supercond.* **26**:1–4. DOI:https://doi.org/10.1109/TASC.2016.2514265.
189. Lambrinos, A., Schaink, A.K., Dhalla, I. et al. (2016). Mechanical thrombectomy in acute ischemic stroke: a systematic review. *Can. J. Neurol. Sci.* **43**:455–460. DOI:https://doi.org/10.1017/cjn.2016.30.
190. Nelson, B.J., Bendok, B.R., Turcotte, E.L. et al. (2024). Remote magnetic navigation enables precision telesurgery. *Sci. Robot.* **9**:eado3187. DOI:https://doi.org/10.1126/scirobotics.ado3187.
191. Li, N., Fei, P., Tous, C. et al. (2024). Human-scale navigation of magnetic microrobots in hepatic arteries. *Sci. Robot.* **9**:eadh8702. DOI:https://doi.org/10.1126/scirobotics.adh8702.
192. Noimark, S., Dunnill, C.W., Wilson, M. et al. (2009). The role of surfaces in catheter-associated infections. *Chem. Soc. Rev.* **38**:3435–3448. DOI:https://doi.org/10.1039/B908260C.
193. Liu, L., Yu, H., Wang, L. et al. (2024). Heparin-network-mediated long-lasting coatings on intravascular catheters for adaptive antithrombosis and antibacterial infection. *Nat. Commun.* **15**:107. DOI:https://doi.org/10.1038/s41467-023-44478-3.
194. Leslie, D.C., Waterhouse, A., Berthet, J.B. et al. (2014). A bioinspired omniphobic surface coating on medical devices prevents thrombosis and biofouling. *Nat. Biotechnol.* **32**:1134–1140. DOI:https://doi.org/10.1038/nbt.3020.
195. Yang, L., Zhang, T., Tan, R. et al. (2022). Functionalized spiral-rolling millirobot for upstream swimming in blood vessel. *Adv. Sci.* **9**:2200342. DOI:https://doi.org/10.1002/advs.202200342.
196. Giaouris, E., Chapot-Chartier, M.-P. and Briandet, R. (2009). Surface physicochemical analysis of natural lactococcus lactis strains reveals the existence of hydrophobic and low charged strains with altered adhesive properties. *Int. J. Food Microbiol.* **131**:2–9. DOI:https://doi.org/10.1016/j.ijfoodmicro.2008.09.006.
197. Walker, D.A., Kowalczyk, B., de la Cruz, M.O. et al. (2011). Electrostatics at the nanoscale. *Nanoscale* **3**:1316–1344. DOI:https://doi.org/10.1039/C0NR00698J.
198. Mu, Q., Jiang, G., Chen, L. et al. (2014). Chemical basis of interactions between engineered nanoparticles and biological systems. *Chem. Rev.* **114**:7740–7781. DOI:https://doi.org/10.1021/cr400295a.
199. Wang, B., Chan, K.F., Yuan, K. et al. (2021). Endoscopy-assisted magnetic navigation of biohybrid soft microrobots with rapid endoluminal delivery and imaging. *Sci. Robot.* **6**:eabd2813. DOI:https://doi.org/10.1126/scirobotics.abd2813.
200. Liu, B., Xu, Z., Gao, H. et al. (2020). Stiffness self-tuned shape memory hydrogels for embolization of aneurysm. *Adv. Funct. Mater.* **30**:1910197. DOI:https://doi.org/10.1002/adfm.201910197.
201. Mura, S., Nicolas, J. and Couvreur, P. (2013). Stimuli-responsive nanocarriers for drug delivery. *Nat. Mater.* **12**:991–1003. DOI:https://doi.org/10.1038/nmat3776.
202. Cao, C., Mou, F., Yang, M. et al. (2024). Harnessing disparities in magnetic microswarms: from construction to collaborative tasks. *Adv. Sci.* **11**:2401711. DOI:https://doi.org/10.1002/advs.202401711.
203. Liu, J., Li, L., Cao, C. et al. (2023). Swarming multifunctional heater–thermometer nanorobots for precise feedback hyperthermia delivery. *ACS Nano.* **17**:16731–16742. DOI:https://doi.org/10.1021/acsnano.3c03131.
204. Wang, Q. and Zhang, L. (2021). External power-driven microrobotic swarm: from fundamental understanding to imaging-guided delivery. *ACS Nano.* **15**:149–174. DOI:https://doi.org/10.1021/acsnano.0c07753.
205. Wang, Q., Wang, B., Chan, K. et al. (2025). Rapid blood clot removal via remote delamination and magnetization of clot debris. *Adv. Sci.* 2415305. DOI:https://doi.org/10.1002/advs.202415305.